ASTRONOMY & ASTROPHYSICS
SUPPLEMENT SERIES

FEBRUARY I **2000**, PAGE 385

Astron. Astrophys. Suppl. Ser. **141**, 385–408 (2000)

A neutral hydrogen survey of polar ring galaxies

III. Nançay observations and comparison with published data

W. van Driel[1], **M. Arnaboldi**[2,3], **F. Combes**[4], **and L.S. Sparke**[5]

[1] Unité Scientifique Nançay, USR CNRS B704, Observatoire de Paris, 5 place Jules Janssen, F-92195 Meudon, France
[2] Osservatorio Astronomico di Capodimonte, V. Moiariello 16, I-80131 Napoli, Italy
[3] Mt. Stromlo and Siding Spring Observatories, Canberra, Australia
[4] DEMIRM, Observatoire de Paris, 61 Av. de l'Observatoire, F-75014 Paris, France
[5] Astronomy Department, University of Wisconsin-Madison, 475 N. Charter St., Madison, WI 53706, U.S.A.

Received January 12; accepted November 8, 1999

Abstract. A total of 50 optically selected polar ring galaxies, polar ring galaxy candidates and related objects were observed in the 21-cm H I line with the Nançay decimetric radio telescope and 31 were detected. The objects, selected by their optical morphology, are all north of declination $-39°$, and generally relatively nearby ($V<$ 8000 $\mathrm{km\,s^{-1}}$) and/or bright ($m_B < 15.5$). The H I line data are presented for all 74 galaxies observed for the survey with the Effelsberg, Green Bank or Nançay radio telescopes, as well as all other published H I line parameters of these objects. Three objects were observed and detected by us at Parkes. A total of 59 objects were detected. For each object a brief description is given based on a literature search.

Key words: galaxies: distances and redshifts — galaxies: general — galaxies: ISM — radio lines: galaxies

1. Introduction

A polar-ring galaxy (hereafter referred to as PRG) consists of a flattened galaxy with an outer ring of gas, dust, and stars rotating in a plane approximately perpendicular to the central disc. Kinematically confirmed PRGs with a disc-dominated central galaxy tend to have wide, extended polar rings, while bulge-dominated objects show only short, narrow rings (Reshetnikov & Sotnikova 1997; Whitmore 1991). The PRGs probably represent merger products, and their study may give us valuable clues about the process and frequency of merging; their visible environment appears to be similar to that of normal galaxies (Brocca et al. 1997), which may support long formation and evolution times of the rings. In addition, measurement of rotation in the two nearly perpendicular planes of the ring and galaxy provide one of the few available probes of the three-dimensional shape of galactic gravitational potentials, and hence the shape of dark and luminous matter distributions.

The PRG catalogue of Whitmore et al. (1990, hereafter PRC) provides us with over a hundred known polar-ring galaxies and PRG candidates, as well as list of possibly related systems, divided into four main categories (number of objects per category from PRC):

1. A: Kinematically-determined Polar-Ring Galaxies (9 objects);
2. B: Good Candidates for Polar-Ring Galaxies (24 objects);
3. C: Possible Candidates for Polar-Ring Galaxies (73 objects);
4. D: Systems Possibly Related to Polar-Ring Galaxies (51 objects).

Since the publication of the PRC, 4 category B and 4 category C objects have been promoted to category A (B–03 = IC 1689, B–17 = UGC 9562, B–19 = AM 2020–504, B–21 = ESO603–G21, C–13 = NGC 660, C–24 = UGC 4261, C–27 = UGC 4385 and C–45 = NGC 5128; see Reshetnikov & Combes 1994; Reshetnikov & Sotnikova 1997; van Driel et al. 1995), all of which are included in our survey and will be considered members of the A category in this paper.

The scientific goals of our 21-cm H I line surveys of PRGs, presented here and in a previous paper (Richter et al. 1994, Paper I) are to:

1. Establish redshifts for the objects with previously unknown redshift;

Send offprint requests to: W. van Driel,
e-mail: Wim.vanDriel@obspm.fr

2. Measure the amount of neutral hydrogen in these systems and examine its correlations with other observational parameters;
3. Identify objects for subsequent synthesis mapping; H I maps together with optical line studies will show which of the new morphological candidates are true polar-ring galaxies, and high-resolution maps will allow dynamical modelling.

Detailed observations of PRGs in the 21-cm H I line with large radio synthesis telescopes like the Australia Telescope, VLA or Westerbork, are crucial for an understanding of the dynamical state of these systems (see, e.g., Schechter et al. 1984; van Gorkom et al. 1989; Cox 1996; Arnaboldi et al. 1997; and the Catalogue of H I maps by Martin 1998). Such mapping measures the distribution and the velocity field of gas in the rings, both of which are required for accurate determination of the shape of the dark halo. Together with optical absorption-line studies of the central galaxy, rotation in the ring gas determines whether morphological candidates are true polar rings. Further, knowledge of the ring mass is necessary to assess the stability of the rings against differential precession, an important consideration in estimating the time since its formation.

Thus, the main purpose of the single-dish H I line surveys of PRGs presented here and in two previous papers is to enlarge the sample of polar-ring systems with sufficient H I gas to allow high-resolution synthesis mapping. After having first observed a sample of 47 PRGs in the 21-cm H I line with the 140-foot (43-m) Green Bank telescope (Paper I), and a sample of 44 with the 100-m Effelsberg telescope (Huchtmeier 1996, Paper II), we now present observations of a similar sample of 50 PRGs with the 94-m diameter equivalent Nançay decimetric radio telescope and of 3 objects observed with the 64-m Parkes dish. An analysis of all available H I data on PRGs and related objects will be presented in the next paper in these series (van Driel et al., in preparation).

In Sect. 2 the sample of PRGs observed in Nançay is presented. In Sect. 3 the results of the Nançay H I observations are shown and compared to H I line observations made elsewhere, either for our PRG survey or for other studies.

2. The Nançay polar-ring galaxy sample

Listed in Table 1 are basic optical data for all 74 galaxies observed for our PRG H I survey at either Green Bank, Effelsberg or Nançay. These data, compiled from many sources, by no means form a homogeneous set. The sources used, in order of preference, are the RC3 (de Vaucouleurs et al. 1991), the online NASA/IPAC Extragalactic Database (NED) and Lyon-Meudon Extragalactic Database (LEDA), and the PRC. The optical systemic velocities listed are mean, weighted and corrected values from the LEDA database, with their quoted error, σ_V. Redshifts for B–10, B–13 and B–14 are by Sackett & Jarvis (private comm.). Note that all radial velocities listed in this paper are heliocentric and calculated according to the conventional optical definition ($V = c(\lambda - \lambda_0)/\lambda_0$). The total blue magnitudes are sometimes indicative only, as they cannot be assumed to be on the same scale, nor do all represent the true total apparent blue magnitude, $B_{\rm T}$, as defined in, e.g., the RC3; sometimes a magnitude measured within a single aperture is used instead. Neither do the measured diameters represent a homogeneous set of measurements, as they sometimes refer to the size of the faint polar ring, and sometimes to the size of the brighter equatorial disc.

A total of 50 polar ring galaxies and PRG candidates from the PRC were observed in the 21-cm H I line at Nançay (see Table 1). Most were selected following essentially the same criteria used for the Green Bank H I line survey (Paper I):

1. Declination north of –39°, and satisfying one or more of the following criteria;
2. Known redshift, less than 8000 $\rm km\,s^{-1}$, or;
3. Blue magnitude brighter than 15.5 mag, or;
4. Member of PRC category A or B (i.e., kinematically confirmed or good candidate).

Of the objects selected using these criteria, 10 were not observed at Nançay, since the properties of their strong H I lines were already well established. These objects are A–03 (NGC 2685), B–11 (UGC 5600), B–17 (UGC 9562), C–13 (NGC 660), C–27 (UGC 4385), C–29 (NGC 2865), C–44 (NGC 5103), C–69 (NGC 7468), D–30 (ESO 341–IG4), and D–35 (NGC 7252).

In addition, we observed one object (A1254–1230) recognized (Schechter et al. 1993) as a good PRG candidate after publication of the PRC, as well as 5 B-category objects of unknown redshift at the start of the Nançay survey: B–8 (AM 0623-371), B-10 (A 0950–2234), B–12 (ESO 503–G17), B–13 (Abell 1631–14) and B–14 (Abell 1644–105).

Note that at Nançay, we could not observe the 8 southernmost objects from the Green Bank survey, due to the smaller range in declination (north of $-39°$) for the Nançay telescope, compared to the limit of $\delta = -45°$ at Green Bank: A–05 (NGC 4650A), B–27 (ESO 293–IG17), C–11 (NGC 625), C–14 (NGC 979), C–42 (NGC 4672), C–45 (NGC 5128), C–48 (ESO 326–IG6), and D–04 (ESO 296–G11).

3. Observations and results

3.1. Nançay and Parkes H I line observations

The Nançay telescope is a meridian transit-type instrument of the Kraus/Ohio State design, consisting of a fixed spherical mirror, 300 m long and 35 m high, a tiltable flat

Table 1. Optical data for the combined polar ring galaxy H I survey sample

PRC No.	Name	R.A. (1950.0)	Dec.	$V_{\rm opt}$ [km s^{-1}]	$\pm\sigma_V$	$B_{\rm T}$ [mag]	$D_{\rm opt}$ [′]
Kinematically-determined polar-ring galaxies							
B–03	IC 1689	01 20 57	32 47 28	4557	60	14.68	0.9
A–01	A 0136–0801	01 36 25	−08 01 24			15.82	1.0
C–13	NGC 660	01 40 21	13 23 20	829	37	12.02	8.3
A–02	ESO 415–G26	02 26 11	−32 06 14	4622	51	14.70	1.3
C–24	UGC 4261	08 07 40	36 58 38	5837	452	14.78	0.9
C–27	UGC 4385	08 21 04	14 54 56	1969		14.51	0.9
A–03	NGC 2685	08 51 41	58 55 30	871	34	12.12	4.5
A–05	NGC 4650A	12 42 05	−40 26 35	2807	100	14.27	1.6
C–45	NGC 5128	13 22 32	−42 45 30	540	66	7.84	25.7
B–17	UGC 9562	14 49 13	35 44 53	1272	60	14.41	1.0
A–06	UGC 9796	15 14 00	43 22 00	5606	60	16.04	1.4
B–19	AM 2020–504	20 20 14	−50 48 48	4963		14.5	
B–21	ESO 603–G21	22 48 41	−20 30 42	3150	60	15.50	1.1
Good candidates for polar-ring galaxies							
B–01	IC 51	00 43 53	−13 42 58	1758	42	13.75	1.3
B–08	AM 0623–371	06 23 07	−37 19 48			16.5	
B–09	UGC 5119	09 34 08	38 19 01	5982	40	14.57	0.7
B–10	A 0950–2234	09 50 35	−22 34 27	14700			
B–11	UGC 5600	10 19 17	78 52 51	2790	82	14.19	1.4
B–12	ESO 503–G17	11 24 24	−27 25 48	10312		16.54	1.3
B–13	Abell 1631-14	12 49 54	−15 36 08	16200		16	0.3
	A1254–1230	12 54 20	−12 29 58	5456		16.1	4
B–14	Abell 1644-105	12 54 59	−16 55 06	15800		16	0.3
B–16	NGC 5122	13 21 36	−10 23 39	2939	31	14.5	0.8
	ESO 235–G58	21 03 03	−48 19 19	4262	42	15.14	2.4
B–20	A 2135–2132	21 35 31	−21 32 41			15.90	0.6
B–23	A 2330–3751	23 30 01	−37 51 09			15.88	
B–24	A 2333–1637	23 33 05	−16 37 14			16.20	1.3
B–27	ESO 293–IG17	23 53 53	−39 26 42	15300	60	16.17	0.8
Possible candidates for polar-ring galaxies							
C–06	NGC 304	00 53 24	23 51 00	4980	53	14.01	1.1
C–09	NGC 442	01 12 05	−01 17 48	5620	50	14.45	1.0
C–11	NGC 625	01 32 55	−41 41 18	391	44	11.71	5.8
C–12	UGC 1198	01 40 58	85 00 38	1207	42	14.80	1.0
C–14	NGC 979	02 29 46	−44 44 38			13.78	1.2
C–18	ESO 358-G20	03 32 53	−32 47 42	1826	50	14.54	1.2
C–25	UGC 4323	08 15 36	67 08 20	3972	55	14.08	1.6
C–26	UGC 4332	08 16 48	21 16 00	5505	94	14.82	1.3
C–28	NGC 2748	09 08 03	76 40 53	1456	58	12.4	3.0
C–29	NGC 2865	09 21 15	−22 56 47	2612	29	12.57	2.5
C–30	UGC 5101	09 32 05	61 34 33	11919	214	14.72	1.1
C–32	IC 575	09 52 04	−06 37 00	5849	95	14.5	1.7
C–33	ESO 500-G41	10 24 34	−23 50 03	3541	35	14.19	1.1
C–34	NGC 3384	10 45 38	12 53 34	735	36	10.85	5.5
C–35	NGC 3414	10 48 31	28 14 24	1445	63	11.96	3.5
C–37	UGC 6182	11 05 08	53 53 13	1255	50	14.12	0.9
C–38	NGC 3934	11 49 38	17 07 44	3697	87	14.28	1.1
C–39	NGC 4174	12 09 54	29 25 00	4010	73	14.31	0.8
C–41	IC 3370	12 24 57	−39 03 42	2935	26	11.99	2.9
C–42	NGC 4672	12 43 30	−41 26 00	3357	62	14.09	2.0
C–44	NGC 5103	13 18 18	43 20 45	1283	50	13.60	1.4
C–46	ESO 576-G69	13 27 22	−20 40 32	5336	60	14.60	1.3:

Table 1. continued

PRC No.	Name	R.A. (1950.0)	Dec.	$V_{\rm opt}$ [km s^{-1}]	$\pm\sigma_V$	$B_{\rm T}$ [mag]	$D_{\rm opt}$ [′]
Possible candidates for polar-ring galaxies – continued							
C–48	ESO 326–IG6	14 08 05	−39 52 15	8598	45	15.0	1.7
C–49	NGC 6028	15 59 16	19 29 52	4480	67	14.35	1.3
C–50	UGC 10205	16 04 36	30 14 06	6605	50	14.4	1.4
C–51	NGC 6285	16 57 36	59 03 00	5580	60	14.80	1.2
	NGC 6286	16 57 45	59 00 43	5606	38	14.36	1.3
C–60	ESO 464–G31	21 15 25	−27 33 35			15	0.6
C–64	ESO 343–IG13	21 33 05	−38 46 06	5710	88	14.55	1.5
C–69	NGC 7468	23 00 30	16 20 04	2105	70	14.16	0.9
Systems possibly related to polar-ring galaxies							
D–02	NGC 235	00 40 24	−23 48 55	6664	48	14.08	1.3
D–03	ESO 474–IG28	00 45 06	−23 04 24	6780	60	14.91	0.7
D–04	ESO 296–G11	01 17 43	−41 29 55	5056	22	14.41	1.0
D–12	UGC 4892	09 13 32	45 54 34			14.8	1.2
D–14	UGC 5485	10 07 40	65 31 23			15.1	1.2
D–15	NGC 3310	10 35 40	53 45 46	1018	26	10.95	3.1
D–16	NGC 3406	10 48 45	51 17 15	7368	225	14.10	1.1
D–19	NGC 3808	11 38 07	22 42 18	7050	38	14.1	1.7
D–21	UGC 7636	12 27 28	08 12 20	276	60	14.80	1.1
D–22	NGC 4643	12 40 47	02 15 06	1328	67	11.72	3.1
D–23	NGC 4753	12 49 48	−00 55 48	1153	186	10.85	6.0
D–24	ESO 575–G44	12 57 41	−22 25 36	9066	90	13.53	1.1
D–25	UGC 8387	13 18 17	34 24 03	6878	68	14.40	1.5
D–28	NGC 6240	16 50 28	02 29 06	7360	77	13.8	2.1
D–30	ESO 341–IG4	20 37 59	−38 22 20	6032	50	13.38	1.9
D–35	NGC 7252	22 17 58	−24 55 51	4767	77	12.47	1.9
D–43	ESO 510–G13	13 52 14	−26 32 18	3467	94	13.35	1.9
D–44	NGC 520	01 22 00	03 31 54	2172	196	12.05	6.8
D–46	NGC 5544	14 14 56	36 48 11	3106	75	14	1.0

Notes: PRC, Polar Ring Catalog number (Whitmore et al. 1990).

mirror (200×40 m), and a focal carriage moving along a 90 m long curved rail track, which allows the tracking of a source on the celestial equator for about 1 hour. Located in the centre of France, it can reach declinations as low as −39°. It has an effective collecting area of roughly 7000 m^2 (equivalent to a 94-m diameter parabolic dish). Due to the elongated geometry of the mirrors, at 21-cm wavelength it has a half-power beam width of 3′.6 E-W× 22′ N–S at declinations from −38° to 15°, and its HPBW in declination increases to 23′ at $\delta = 30°$, 25′.5 at 50° and 32′.5 at 70° (E. Gérard, private comm.). Typical system temperatures were ∼40 K for our project.

The observations at Nançay were made during several observing runs in the period of July 1995–July 1998, using a total of about 340 hours of telescope time. For a technical description of the Nançay decimetric radio telescope and the general methods for data handling and reduction see, e.g., Theureau et al. (1998) and references therein. Most objects were observed for about four 1-hour long periods; one hour being the typical maximum tracking time for the transit-type Nançay telescope. We obtained our observations in total power (position-switching) mode using consecutive pairs of two-minute on- and two-minute off-source integrations. Off-source integrations were taken approximately 20$^{\rm m}$ E of the target position. For objects with known redshifts the autocorrelator was divided into two pairs of cross-polarized receiver banks (H and V polarisation), each with 512 channels and a 6.4 MHz bandpass, and the centre frequencies of the two banks were tuned to the redshifted systemic H I velocity of the target measured in the Green Bank survey (Table 2), if known, or on the optical systemic velocity (Table 1), if not. Thus, the velocity coverage is about 1200 km s^{-1} with a velocity resolution of about 3.1 km s^{-1}. For the determination of the H I line profile parameters and upper limits (see Table 2), the velocity resolution was degraded to 15.8 km s^{-1}.

For the 8 objects that had no known redshift at the start of the Nançay survey (B–08, 10, 13, 14, 20, 23, 24, and D–14), the autocorrelator was divided into four slightly overlapping banks of 256 channels each. Thus, a

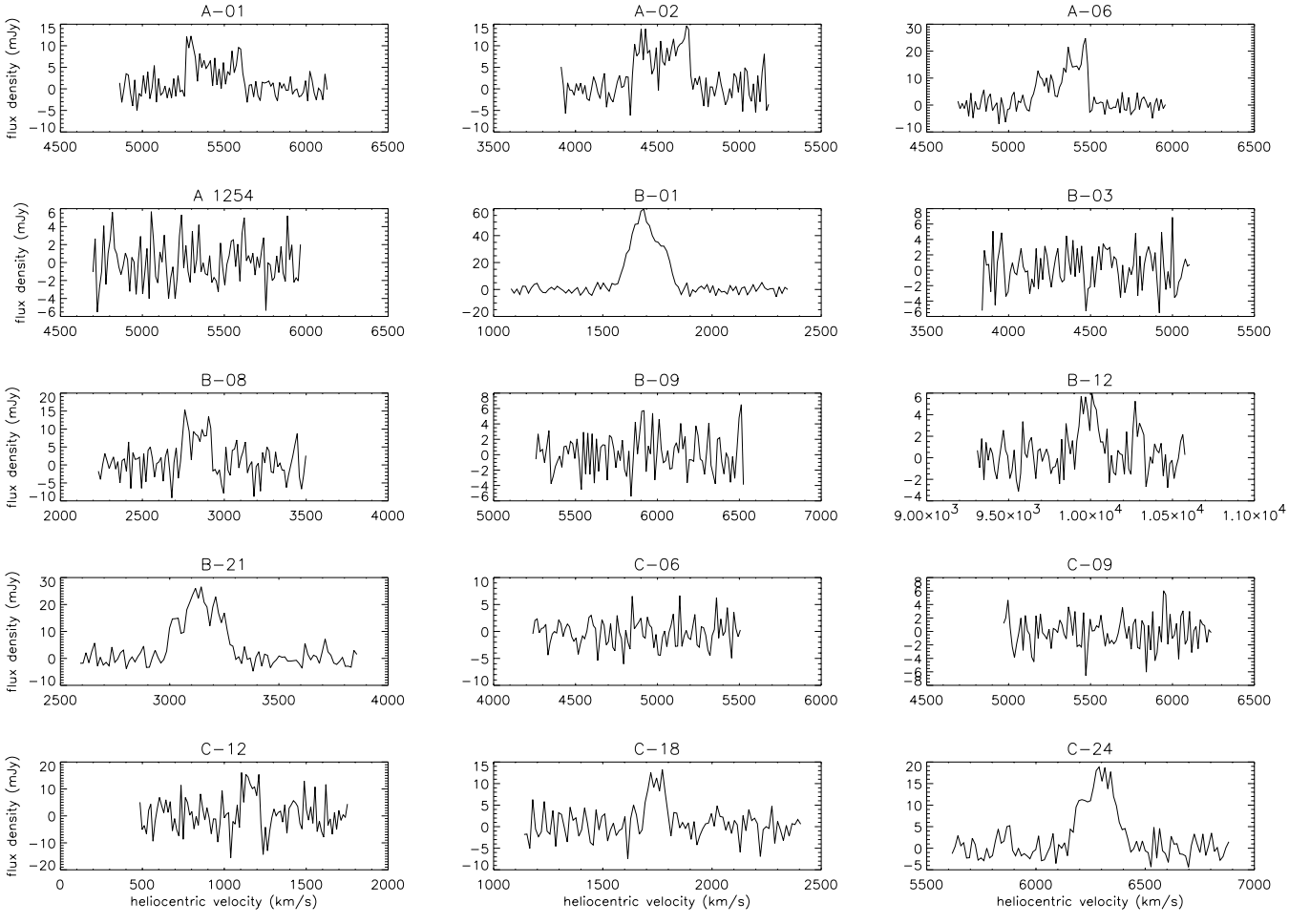

Fig. 1. a) 21-cm H I line spectra of all polar-ring galaxies and polar ring galaxy candidates with previously known redshift observed at Nançay, and of PRC B–08, whose redshift was first measured in the present survey, as well as of PRC D–14, whose redshift was unknown when it was observed for the survey. Velocity resolution is 15.8 $\mathrm{km\,s^{-1}}$ for all spectra, except for PRC D–14, where it is 19.0 $\mathrm{km\,s^{-1}}$. Radial velocities are according to the radio convention

search for H I line emission was made in the H polarization channel only, separately in two velocity ranges, $340 - 5207$ $\mathrm{km\,s^{-1}}$ and $5140 - 10007$ $\mathrm{km\,s^{-1}}$, respectively. The velocity resolution used for the determination of the profile parameters or upper limits (Table 3) was 19.0 $\mathrm{km\,s^{-1}}$; the two upper limits given in Table 3 for undetected objects of unknown redshift represent, respectively, the two aforementioned velocity search ranges. Subsequently, one object detected in this mode, B–08, was reobserved in the same way as the other objects with known redshift.

We reduced our H I spectra using the standard Nançay spectral line reduction packages available at the Nançay site. With this software we subtracted baselines (generally third order polynomials), averaged the two receiver polarizations, and applied a declination-dependent conversion factor to convert from units of T_{sys} to flux density in mJy. The T_{sys}-to-mJy conversion factor is determined via a standard declination-dependent calibration relation established by the Nançay staff through regular monitoring of strong continuum sources. In addition, we applied a flux density scaling factor (see Matthews et al. 1998; Matthews & van Driel 2000) of 1.26 to our spectra based on statistical comparisons of our late-type spiral survey observations with other data. The reduced Nançay spectra are shown in Fig. 1.

In addition, three PRGs were observed and detected with the 64-m Parkes radiotelescope for our survey: B–01 (IC 51), B–19 (AM 2020–504) and B–21 (ESO 603–G21). Of these, B–19 is a southern object out of reach of the other 3 telescopes used for our survey, with no published H I data. The profile parameters derived for these objects are listed in Table 3.

Table 2. H I survey data for the combined polar ring galaxy H I sample

PRC No.	H I Observations Telescope codes Survey	Others	— V_{HI} — Nan	GB [km s^{-1}]	Eff	— $\int S\,dV$ — Nan	GB [Jy km s^{-1}]	Eff	— ΔV_{20} — Nan	GB [km s^{-1}]	Eff	ΔV_{50} Nan [km s^{-1}]	rms Nan [mJy]
Kinematically-determined polar-ring galaxies													
A–01	E,G,N	V	5537	5521	5670	2.07	3.82	3	360	408	310	346	2.2
A–02	G,N	V	4596	4572		3.16	6.22		359	441		347	3.0
A–03	G	E,G,G43,N,W		875			34.2			298			
A–05	G	AT,P,V		2909			23.2			244			
A–06	E,G,N	V,W	5424	5480	5423	4.94	16.4	7.3	343	354	214	314	2.9
B–03	N	A,V	—			<2.1			—				2.3
B–17	G	A,N,W		1239			13.6			200			
B–21	E,G,N	P	3165	3180	3449	4.95	14.3	17.2	286	272	355	251	2.6
C–13	G	A,G,G43,N,W		848			187.8			325			
C–24	E,G,N	A	6411	6410	6404	2.32	4.62	3	241	241	239	188	2.3
C–27	E,G	A		1954	1968		7.93	7.4		196	177		
C–45	G	P,R		524			300			570			
Good candidates for polar-ring galaxies													
B–01	E,G,N	P	1715	1709	1728	9.1	11.5	9.4	242	253	236	169	2.6
B–08	N		2859			1.69			188			178	3.9
B–09	N,E		—		5856	<2.4		7	—		353		2.3
B–10*	E,N		—			<2.8/2.6			—				2.7/2.5
B–11	E,G	G		2769	2769		12.0	11.1	—	173	156		
B–12	G,N		10481	—		1.46	<6.0		415	—		377	1.5
B–13*	N		—			<4.6/4.6		—	—				3.6/3.6
A1254	N		—			<2.1			—				2.3
B–14*	N		—			<4.5/5.0		—	—				3.5/3.9
B–16	E	V			2842			5.4			386		2.2
B–20	N		—			<2.3/2.8			—				3.1/3.7
B–23	G,N	P	—	—		<4.3/3.2	<2.2		—	—			5.7/4.2
B–24	N		—			<2.9/2.1			—				2.9/2.8
B–27	G			—			<3.7			—			
Possible candidates for polar-ring galaxies													
C–06	N	A	—			<2.9			—	—			2.4
C–09	E,G,N		—	5629	—	<2.4	1.53	<3.2	—	302	—		2.3
C–11	G	G43,P		394			37.4			113			
C–12	E,G,N		1162	1149	1152	0.87	1.64	3.6	143	174	152	117	5.4
C–14	G	P		4775			26.2			678:			
C–18	G,N	N	1753	1799		1.08	1.75		114	167		94	2.9
C–25	E,G,N		—	3686	4037	<3.4	3.56	0.9	—	397	250		3.8
C–26	E,G,N	A		5811	5412	<2.8	3.96	4.3	—	299	620		3.1
C–28	E,N	G,E,J,W	1479		1478	34.39		54	313		140	291	4.8
C–29	E,G	E		2772	2850		2.9	1.7		164	159		
C–30	E,N		12053		—	-1.2:		<2.7	189		—	152	3.9
C–32	E,N		—		6639	<3.3		1.6	—		273		2.9
C–33	E,N		3560		3570	2.94		5	237		332	218	2.8
C–34	N	A	903			1.47			93			41	2.1
C–35	E,G,N	A	1173	—	1526	2.97	<7.8	1.2	325:	—	322	175	1.8
C–37	E,G,N	G	1228		1255	10.47		10.7	90		114	86	4.0
C–38	E,G,N	A	3768	3793	3702	8.73	5.71	15.9	367:	91	317	227:	2.2
C–39	E,G,N	A	3842:	3811	3936	5.17	12.9	9.4	413	439	262	191	3.6
C–41	G,N		—	3219		<2.8	1.42		—	92			3.1
C–42	G	P		3242			7.67			401			
C–44	E,G	G		1289	1288		6.76	3.5		141	141		
C–46	E,G,N	N	—	5759	5365	<2.8	2.91	4.6	—	109	464		3.1

Table 2. continued

PRC No.	H I Observations Telescope codes Survey	Others	— V_{HI} — Nan	GB	Eff	— $\int S\,dV$ — Nan	GB	Eff	— ΔV_{20} — Nan	GB	Eff	ΔV_{50} Nan	rms Nan
			[km s^{-1}]			[Jy km s^{-1}]			[km s^{-1}]			[km s^{-1}]	[mJy]
Possible candidates for polar-ring galaxies – continued													
C–48	G			—			<10.7			—			
C–49	E,N	A	4470		4474	2.07		1.1	303		293	262	2.3
C–50	E,G,N	N	6559	6773	6560	2.43	1.96	3.9	540:	163	595	517	2.6
C–51	E,G,N	G	5497	—	—	1.40	<4.8	<3.4	184:	—	—	174:	4.1
C–60	E,G,N		—	6529	—	<2.6	5.42	<4.5	—	573	—		2.9
C–64	G,N		5696	5716		2.18	4.55		269	342		217	4.5
C–69	G	A,E,N,V		2072			16.1			247			
Systems possibly related to polar-ring galaxies													
D–02	E,G,N		6748	6710	6765	1.37	2.84	2.4	243	282	303	212	2.8
D–03	E,G,N		6614	6610	6635	1.55	2.62	3	136	220	135	75	2.6
D–04	G			5162			14.0			442			
	G			5593			1.38:			167:			
D–12	E,N		7778		—	2.13		<3.7	283		—	267	2.4
D–14	E,N		5985		5990	13.82		16.2	395		331		6.2/7.9
D–15	E	A,E,G,N,W			983			54.4			234		
D–16	E,N		—		—	<4.0		<8.3	—		—		3.3
D–19	N	A	7072			1.88			270			252	2.3
D–21*	E,N	A	(471		475	0.59		0.63	48		47	33)	2.7
D–22	E,G,N	A	1327	1053	1325	1.58	3.20	2.3	293	141	274	257	2.1
D–23	E,N	G,G43,P	—		1396	<1.9		0.55			91		2.1
D–24*	E				2806			1			390		
D–25	E,G,N	A	—	7024	—	<4.0	2.95	<2.9		279	—		3.3
D–28	E,G,N	A,V	7272	7197	—	-0.7:	3.78	<5.9	198	616	—	165	2.2
D–30	G			6055			9.05			284			
D–35	E,G	G43,N,V		4752	4750		4.58	3.8		191	223		
D–43	E,G,N	N	3451	—	3452	5.85	<10.0	3.1	573	—	571	559	2.2
D–44	E	A,G,G43,J,N			2189			21.3			450		
D–46	E	A,G			3078			2.2			234		

Notes: N/Nan = Nançay, G/GB = Green Bank, and E/Eff = Effelsberg data, for other telescope codes: see Sect. 3.2 and footnote to Table 3; — means no detection. Upper limits to the integrated line flux $\int S\,dV$ are 3σ values for linewidths depending on luminosity, see text. * B–10, B–13 and B–14: have redshifts outside the H I search range; D–21 and D–24: these detections are unrelated to the PRC objects.

3.2. Notes to individual galaxies

Here we give detailed notes on all objects observed at Nançay, as well as on other objects for which the Green Bank and Effelsberg data show discrepant H I velocities, line widths, or integrated line fluxes. We have indicated for each object with which telescopes it has been observed for our PRG H I survey, or for other projects (see also Table 3): A = Arecibo 305-m, AT = Australia Telescope, E = Effelsberg 100-m, G = Green Bank 90-m, G43 = Green Bank 43-m, IAR = I.A.R. 30-m, N=Nançay 94-m equiv., J = Jodrell Bank 76-m, P = Parkes 64-m, R = RATAN 600, V = VLA and W = Westerbork. The listed upper limits to the integrated H I line flux are 3σ limits for flat-topped profiles using estimated widths depending on the blue luminosity of the galaxies. The linewidths of detected PRC objects show an increase with luminosity (van Driel et al., in prep.), though with large scatter. We used the average ΔV_{20} linewidth for a given L_B. Consequently, the listed upper limits for the Green Bank and Effelsberg non-detections are different from those quoted in Papers I and II, where a linewidth of 250 km s^{-1} was assumed for all objects. For the 3 non-detected objects without known blue luminosity (B–20, B–23 and B–24) a linewidth of 250 km s^{-1} was assumed, being the average of all detected objects in the sample.

Photographs of Schmidt telescope sky survey-quality of all objects can be found in PRC, and explicit reference is made only to images published elsewhere.

The following data on possible companions detectable within the Nançay beam were extracted from the NED and LEDA database, searching in an area of $5' \times 28'$ ($\Delta\alpha \times \Delta\delta$), i.e. 1.25 times the $4' \times 22'$ Nançay HPBW in R.A. and in Dec, centered on the pointing positions of the telescope (see Table 1). A search for nearby optical companions of many PRGs was made by Brocca et al. (1997).

Kinematically confirmed PRGs

A–01 = A0136–0801. (E,G,N,V) Well-studied object with a polar ring extending to about three times the radius of the equatorial disc; for images, surface photometry and spectra: see Schweizer et al. (1983), Reshetnikov et al. (1994). Listed as one of the disc-dominated PRGs with large polar rings by Reshetnikov & Sotnikova (1997). Mapped in H I with the VLA by Cox et al. (1995) and van Gorkom et al. (1987), who detected an integrated H I line flux of 1.1 and 2.9 Jy km s^{-1}, respectively. All H I emission is found to be associated with the polar ring, whose outer H I contours appear to warp away from the poles. The H I distribution and velocity field are quite regular, indicating an old and possibly stable ring. The central stellar velocity dispersion is 67 km s^{-1} (Schweizer et al. 1983; Whitmore et al. 1987). No other galaxies were found within the Nançay search area.

A–02 = ESO 415–G26. (G,N,V) Its polar ring is less extended than the stellar disc in optical images; it has extensive debris at a position angle intermediate between those of the disc and the ring, as well as shells and loops in the outer regions - see Schweizer et al. (1983), van Gorkom et al. (1987), Whitmore et al. (1987) and Reshetnikov et al. (1994). Listed as one of the bulge-dominated PRGs with short, narrow rings by Reshetnikov & Sotnikova (1997). Mapped with the VLA by van Gorkom et al. (1987), who detected 3.2 10^9 $M_\odot$ of H I. Both Nançay and Green Bank profiles, centered at 4665 km s^{-1} and 400 km s^{-1} wide, could be confused by the very nearby (0.′1 separation) galaxy [RC3] 022508–315509 at 4530 ± 15 km s^{-1}, within the linewidth of the PRG. No other galaxies were found within the Nançay search area.

A–06 = UGC 9796 = II Zw 73. (E,G,N,V,W) Very faint polar ring, whose Hα kinematics show it to be actually a differentially rotating disc, about 25° from perpendicular to the equatorial disc; No nuclear Hα emission (Reshetnikov & Combes 1994). Images, surface photometry: see Reshetnikov et al. (1994), Reshetnikov & Combes (1994) and PRC; optical rotation curve: see Makarov et al. (1997). Listed as one of the disc-dominated PRGs with large polar rings by Reshetnikov & Sotnikova (1997). Since the Green Bank and Effelsberg profiles look quite different, the galaxy was also observed at Nançay. VLA imaging observations (Cox et al. 1995; van Gorkom et al. 1987) show that all our single-dish spectra are confused by companion galaxies, however; for example, 7 companions were detected at the VLA within the Green Bank beam area, resulting in a integrated H I line flux 5 times higher than that of the PRG itself. The VLA images show that in the PRG all H I emission is associated with the polar ring, whose outer H I contours appear to warp away from the poles, in the same sense as the optical warp. No sign of interaction was found between the PRG and its close companion, MCG 07–31–049, a 15.7 mag Irregular at $V_{\rm hel} = 5470$ km s^{-1} (63 km s^{-1} higher than that of the PRG) at 1.′4 distance. The only other object within the Nançay search area is a 15.7 mag galaxy pair of 0.′5 diameter with a redshift of 5606 km s^{-1}, at 1.′5 distance.

B–03 = IC 1689. (A,N,V) An S0-type galaxy with a warped disc and a blue *inner* polar disc of only 2 kpc radius. Listed as one of the bulge-dominated PRGs with short, narrow rings by Reshetnikov & Sotnikova (1997). Surface photometry and images: see Hagen-Thorn & Reshetnikov (1997), Reshetnikov et al. (1995), van Gorkom et al. (1987) and the PRC. Two-dimensional spectroscopy of the inner parts (Sil'chenko 1998) shows the orthogonality of star and gas rotation and evidence for a central secondary star formation burst. Not detected at Nançay (line flux <2.1 Jy km s^{-1}), nor at the VLA or Arecibo; best upper limit is 0.55 Jy km s^{-1} (see Table 3), which sets an upper limit of about 5.5 10^8 $M_\odot$ to the H I mass (for $H_0 = 75$ km s^{-1} Mpc^{-1}) and of 0.085 $M_\odot/L_{\odot,B}$ to the $M_{\rm HI}/L_B$ ratio. Four other galaxies were found within the Nançay search area: (1.) IC 1690, a 14.9 mag elliptical at a redshift of 4537 km s^{-1}, at 6.′3 distance, (2.) NPM1G +32.0060 (Klemola et al. 1987), a 15.9 mag elliptical at a redshift of 5158 km s^{-1}, at 9.′1 distance, (3.) the galaxy pair NGC 507/508 (= Arp 229), at an average distance of 13′; NGC 507 is a 12.2 mag early-type spiral of type SA(r)0^0 at a redshift of 4924 km s^{-1}, and NGC 508 is a 14.1 mag probable elliptical at a redshift of 5529 km s^{-1}. They are listed as members of the NGC 507 group of galaxies (Garcia 1993). Though all four have redshifts within the range of the Nançay spectrum ($3970 - 5170$ km s^{-1}), only NGC 507 could be a possible source of confusion, but no line emission was detected from this galaxy. Modelling of its kinematics indicates a flattened dark halo surrounding the PRG.

B–17 = UGC 9562. (A,G,N,V,W) Mapped at the VLA by Cox et al. (1995), who found that the H I is more orderly than earlier low-resolution Westerbork observations (Balkowski 1978) suggested. There is a long streamer of gas connecting the ring spatially and in velocity with II Zw 70, a star-forming dwarf galaxy about 4 arcmin away. The streamer of gas and the dwarf II Zw 70 each have about 1/3 of the H I flux from II Zw 71 itself.

B–19 = AM 2020–504. (P) This is the best-studied case to date of a PR around an elliptical: the optical luminosity profile of the central stellar component follows the $R^{1/4}$ law (Arnaboldi et al. 1993a). The optical and K-band imaging of the polar-ring shows a gentle warp: the PR is probably stable, giving time to stars to form

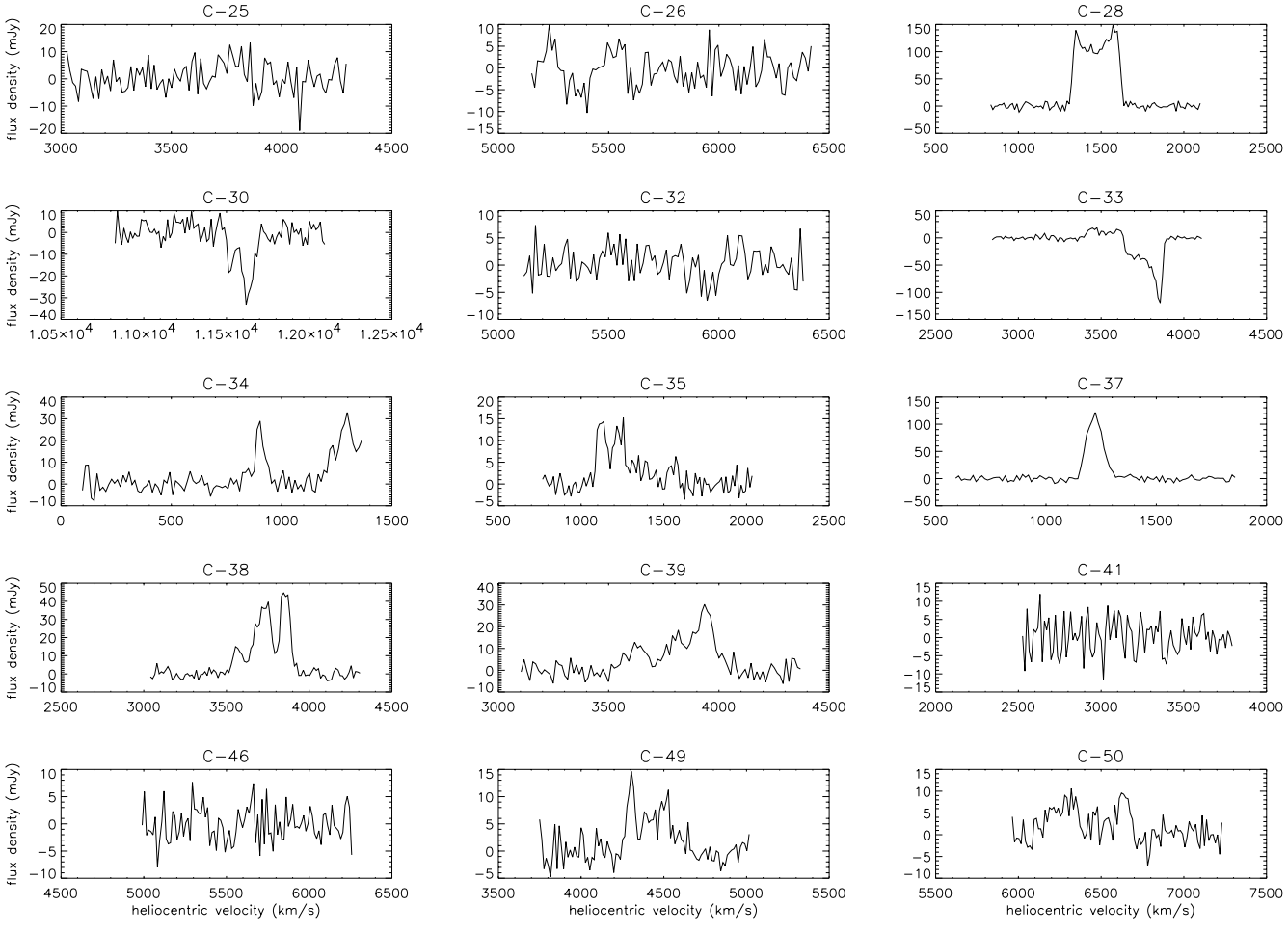

Fig. 1. b) Nançay 21-cm H I line spectra – continued

and grow old. This galaxy has a UV spectrum typical of a starburst galaxy (Arnaboldi et al. 1993b). Our Parkes single dish observations show a total integrated flux of 2.4 Jy $\mathrm{km\,s^{-1}}$, centered at 5181 $\mathrm{km\,s^{-1}}$, with a FWHM of 164 $\mathrm{km\,s^{-1}}$.

B–21 = ESO 603–G21. (E,G,N) This galaxy exhibits a severely warped structure, which appears dark when crossing the stellar central body – photograph: see Schweizer et al. (1983), CCD image: see PRC. Also identified as possible PRG in Buta (1995). The near-infrared imaging in the K-band (Arnaboldi et al. 1995) showed that most of the stellar light comes from a bright nearly-exponential disk in the plane of the warped dusty structure, and the warp is clearly visible in the K-light. The central round body visible in the optical images is quite faint in the near-infrared. Analysis of the K-image showed the presence of a filament perpendicular to the edge-on exponential disk, which is possibly the true polar ring. Our Parkes single dish observations for ESO 603–G21 give a central velocity 3193 $\mathrm{km\,s^{-1}}$, a FWHM of 217 $\mathrm{km\,s^{-1}}$ and a total integrated intensity of 14.4 Jy $\mathrm{km\,s^{-1}}$. The total H I mass associated with this object is 6.2 10^9 $M_\odot$ Since the Green Bank and Effelsberg profiles have a 270 $\mathrm{km\,s^{-1}}$ central velocity difference, the galaxy was also observed at Nançay, where we found a central velocity (3165 $\mathrm{km\,s^{-1}}$) and ΔV_{20} width (286 $\mathrm{km\,s^{-1}}$) similar to the Green Bank results. No other objects were found within the Nançay search area, but the Green Bank and Effelsberg observations are confused by an object at basically the same redshift as B–21: ESO 603–G20, a 14.7 mag edge-on superthin galaxy, located 5′ W of the PRC object, for which a Nançay H I flux of 8.6 Jy $\mathrm{km\,s^{-1}}$ was measured, centered at 3189 $\mathrm{km\,s^{-1}}$ with a FWHM of 216 $\mathrm{km\,s^{-1}}$ (Theureau et al. 1998) – the presence of this object in the beams cannot explain the discrepancy between the Green Bank and Effelsberg profiles, though. No other objects were found within the Nançay search area.

C–24 = UGC 4261. (A,E,G,N) Possibly in the process of forming a ring through accretion (Reshetnikov & Combes 1994). Multicolor surface photometry: Reshetnikov et al. (1998). The Hα rotation curve (Reshetnikov & Combes 1994) along the suspected ring (or, probably, ring in formation) is asymmetric.

Has an H II-type nuclear spectrum (Reshetnikov & Combes 1994; Keel 1985; Weistrop & Downes 1991). One other galaxy was found within the Nançay search area: KUG 0808+370, a 17 mag spiral of unknown redshift, at 8′.8 distance.

Good candidates

A1254–1230. (N) Not in PRC, but identified as good PRG candidate by Schechter et al. (1993), who give an optical redshift. Not detected at Nançay (line flux < 1.7 Jy km s^{-1}). No other galaxies were found within the Nançay search area.

ESO 235–58. (P) This galaxy was erroneously classified as a barred spiral galaxy, with a weak broken ring surrounding a bar, but a later analysis of the optical images showed it to be a polar ring (Buta & Crocker 1993): the un-sharp masking revealed a dust lane along the elongated component, previously identified as a bar, showing it to be an edge-on S0. CCD photometry: Buta & Crocker (1993). Single dish H I observations (Mathewson 1993, private communication) done at Parkes indicated a central velocity of 4310 km s^{-1}, a FWHM of 292 km s^{-1} and a total line flux of 5.8 Jy km s^{-1}.

B–01 = IC51 (E,G,N) The ring has about the same size as the inner component, and the galaxy has an extensive set of distinct outer stellar shells - photos: see Arp (1966) and Hernquist & Quinn (1988); optical and radio imaging: see Mollenhoff et al. (1992); Secondary nucleus - see Forbes et al. (1994). Mapped in H I at the VLA by Schiminovich (see Galletta et al. 1997) who found emission around 1725 km s^{-1} only; the CO and H I may have different kinematics. Our Parkes H I profile shows a detection centered at 1763 km s^{-1}, with a FWHM of 175 km s^{-1} and an integrated line flux of 10.9 Jy km s^{-1}. An H_2 mass of 7 10^8 $M_\odot$ was derived from CO(1-0) line mapping by Galletta et al. (1997), centered at 1666 km s^{-1}. The claim (in Galletta et al. 1997) that our Nançay H I data show detections at other velocities (in the range of 1310–1900 km s^{-1}) is in error; the spectrum presented here is fully consistent with the Green Bank and Effelsberg data.

B–08 = AM 0623–371 (N) Has a small luminous component perpendicular to the main body. This object was first observed in the velocity-search mode (range 340–10007 km s^{-1}) and detected as a weak profile straddling two correlator banks. We therefore reobserved it in the same mode as the other objects with known redshift - the quoted profile parameters (Table 3) are from the latter observations. There are several other objects within the Nançay search area, members of the Abell 3390 cluster at redshifts of about 9500 km s^{-1}, none of which could cause confusion with the H I detection at 2863 km s^{-1}. Note that the reference CSRG 0497 (Buta 1995) refers to the nearby 9745 km s^{-1} object, not to B–08 (though in the NED and LEDA database B–08 and CSRG 0497 are regarded as one and the same object).

B–09 = UGC 5119. (N) Has a very faint, small component perpendicular to the main body. It was not detected at Nançay (line flux <1.7 Jy km s^{-1}), but detected at Effelsberg with a line flux of 7 Jy km s^{-1}, see Paper II where it is erroneously listed as B–10 in Table 1. The Effelsberg spectrum appears affected by strong radio interference, and the "detection" could therefore well be spurious. There are no other published H I observations of this object. Long-slit Hα spectra (Reshetnikov & Combes 1994) show strong line absorption and no nuclear Hα emission. No optical emission lines were found by Osterbrock & Dahari (1983). No other galaxies were found within the Nançay search area.

B–10 = A0950–2234. (E,N) Faint structure perpendicular to the main axis, extending to about twice the radius of the principal disc. Not detected at Nançay (line flux <2.0 Jy km s^{-1}), but the redshift of 14700 km s^{-1} reported by Sackett & Jarvis (private comm.), and unknown at the time of the Nançay observations, lies well outside the velocity search window. Note that the detected object listed as B–10 in Table 1 of Paper II is in fact B–09. This object is not listed in the NED or LEDA database, nor were any other objects found within the Nançay search area.

B–12 = ESO 503–G17. (G,N) One of the best defined polar ring candidates in Category B; the perpendicular structure extends to about twice the radius of the principal disc. The optical redshift is from Jarvis & Sackett (private communication, see Paper I). No other objects were found within the Nançay search area.

B–13 = Abell 1631–14. (N) Faint, broad ring structure inclined about 30° to the minor axis, extended to about twice the radius of the principal disc. Not detected at Nançay (line flux <2.7 Jy km s^{-1}), but the redshift of 16200 km s^{-1} reported by Sackett & Jarvis (private comm.), and unknown at the time of the Nançay observations, lies well outside the velocity search window. Three other members of the Abell 1631 cluster were found within the Nançay search area: Nos. 7, 9 and 10 with redshifts of 14909, 14654 and 14345 km s^{-1} (Dressler & Schectman 1988), respectively. If the PRG is a cluster member its redshift would be well beyond our H I search range of 340 to 10007 km s^{-1}.

B–14 = Abell 1644–105. (N) Ring is too faint to be seen on POSS plates, but CCD imaging shows it to be well-defined and symmetric (PRC). Not detected at Nançay (line flux <2.8 Jy km s^{-1}), but the redshift of 15800 km s^{-1} reported by Sackett & Jarvis (private comm.), and unknown at the time of the Nançay observations, lies well outside the velocity search window. All 5 objects found within the Nançay search area are 15 or 16$^{\rm th}$ mag E or S0 galaxies and members of cluster Abell 1644 (Abell et al. 1989) at a mean redshift of 14213 km s^{-1} (Zabludoff et al. 1993).

B–16 = NGC 5122. (N,V) Listed as one of the disc-dominated PRGs with large polar rings by

Reshetnikov & Sotnikova (1997). Its faint ring is smooth and warped, and very nearly perpendicular to the disc, and both are seen nearly edge-on; CCD image by J. Gallagher & L. Matthews: in Cox et al. (1995). Stellar absorption lines only were found by Rodgers et al. (1978). The galaxy was observed at a higher, *incorrect redshift*, at both Green Bank and Nançay. The galaxy was detected in Nançay at the correct redshift by Theureau et al. (1998), see Table 3; no confusing objects were found within the Nançay search area. Mapped in H I at the VLA (Cox et al. 1995), who found that the H I is associated with the ring, not with the host galaxy. The ring is asymmetric and extends towards a companion galaxy, MCG-02-34-045, a 15.5 mag Sc/d object at $V_{\rm hel} = 2929$ km s^{-1} (74 km s^{-1} higher than that of the PRG) at 11′.6 distance. The polar ring gas is not warped, and no gaseous bridge is visible between the two companion galaxies.

B–20 = A 2135–2132. (N) Not detected at Nançay (line flux <2.5 Jy km s^{-1}). This object is not listed in the NED database, nor were any other objects found within the Nançay search area.

B–23 = A 2330–3751. (G,N) Faint structure perpendicular to the major axis, a bit smaller than the major axis diameter of the principal disc. Spectra were obtained at the Siding Spring Observatory 2.3 m telescope and the double beam spectrograph in August 1995 to get the optical redshift along the PR along PA = 156°. The wavelength range in the blue arm was from 3600 to 5600 Å, and from 6400 to 7005 in the red. No features were indentified upon the continuum emission. Not detected at Nançay or Green Bank (line flux <2.2 Jy km s^{-1}). Only referred to in the PRC and Paper I. The centres of 2 galaxy concentrations lie within the Nançay search area: B–23 is located 5′.7 from the centre of cluster AM 2330–375 (Arp & Madore 1987), and 8′.5 from the centre of cluster Abell 4015, both of unknown redshift.

B–24 = A 2333–1637. (N) Asymmetric polar ring, about 45° from perpendicular – transitory configuration? Not detected at Nançay (line flux <2.5 Jy km s^{-1}). This object is not listed in the NED and LEDA database, nor were any possible companions found within the Nançay search area.

B–27 = ESO 293–IG17. (G) Only a slight extension is seen along the minor axis, appears to be surrounded by shell-like nebulosity. After the completion of our H I survey an optical redshift of about 15300 km s^{-1} was published (Loveday et al. 1996), which places the object well outside the $1000-8000$ km s^{-1} velocity search range used at Green Bank.

Possible PRG candidates

C–06 = NGC 0304. (A,N) Shows faint filaments along the minor axis; it is not clear from surface photometry whether it is an elliptical or a disc system (PRC). Classified by Keel (1985) as an edge-on spiral, based on CCD images. Not detected at Nançay (line flux <2.9 Jy km s^{-1}), nor at Arecibo (see Table 3), giving a best upper limit to the integrated H I line flux of 1.0 Jy km s^{-1}. No other objects were found within the Nançay search area.

C–09 = NGC 0442. (E,G,N) Has a dust lane perpendicular to the major axis, and two short spikes on either side of the galaxy; surface photometry: see PRC. Not detected at Nançay or Effelsberg, but detected at Green Bank. The only other object found within the Nançay search area is IRAS F01119−0128, of unknown redshift, with a flux density of 3.6 Jy at 100 μm wavelength, at a distance of 10′.6.

C–12 = UGC 1198 = VII Zw 3 (E,G,N) Small galaxy, crossed by a slight enhancement of light along its minor axis; surface photometry: see PRC. No other galaxies were found within the Nançay search area.

C–14 = NGC 979 (G) No optical redshift has been published for this object. Our Green Bank H I profile of this galaxy is very broad ($\Delta V_{20} = 678$ km s^{-1}) and centered at 4775 km s^{-1}. This may be due to confusion with ESO 426–22, a 14.8 mag SBc spiral at 9′ distance with an optical redshift of 5127 ± 60 km s^{-1}; no H I spectrum has been published of this galaxy.

C–18 = ESO 358–G20. (G,N) Shows a faint ringlike structure to the north, as well as scattered debris to the southeast and a bright "crescent moon" feature just south of the nucleus. The Green Bank H I profile is considerably wider than the Nançay profile (167 and 114 km s^{-1}, respectively) – due to interference? Our observations, plus 30 minutes more, were used by Matthews et al. (1998). Within the Nançay search area only two probable ellipticals were found of about 19 mag, without known redshift, at an average distance of 12′.5.

C–25 = UGC 4323. (E,G,N) Maybe in the process of forming a ring through accretion (Reshetnikov & Combes 1994), shows a faint jetlike extension to northeast and an inner dust lane near the minor axis. Optical study by Reshetnikov et al. (1995), optical spectrum: see Moody & Kirshner (1988). It's optical redshift is 3972 ± 55 km s^{-1}. Asymmetric Hα rotation curve (Reshetnikov & Combes 1994). Has a LINER-type nuclear spectrum (Reshetnikov & Combes 1994). It was not detected at Nançay (line flux <2.9 Jy km s^{-1}), while the Green Bank and Effelsberg profiles do not even show an overlap in velocity (the measured mean velocities and ΔV_{20} widths are 3686, 397 km s^{-1} and 4037, 250 km s^{-1}, respectively), and the Effelsberg integrated line flux is 4 times smaller than that measured at Green Bank. The complete discrepancy between the two H I spectra, as well as between the Green Bank and optical redshifts appears to be due to interference at Green Bank rather than to confusion with other galaxies in the beams.

C–26 = UGC 4332. (A,E,G,N) Optical and near-infrared imaging: Gavazzi et al. (1994, 1996a); Hubble Space Telescope imaging of central regions: Malkan et al.

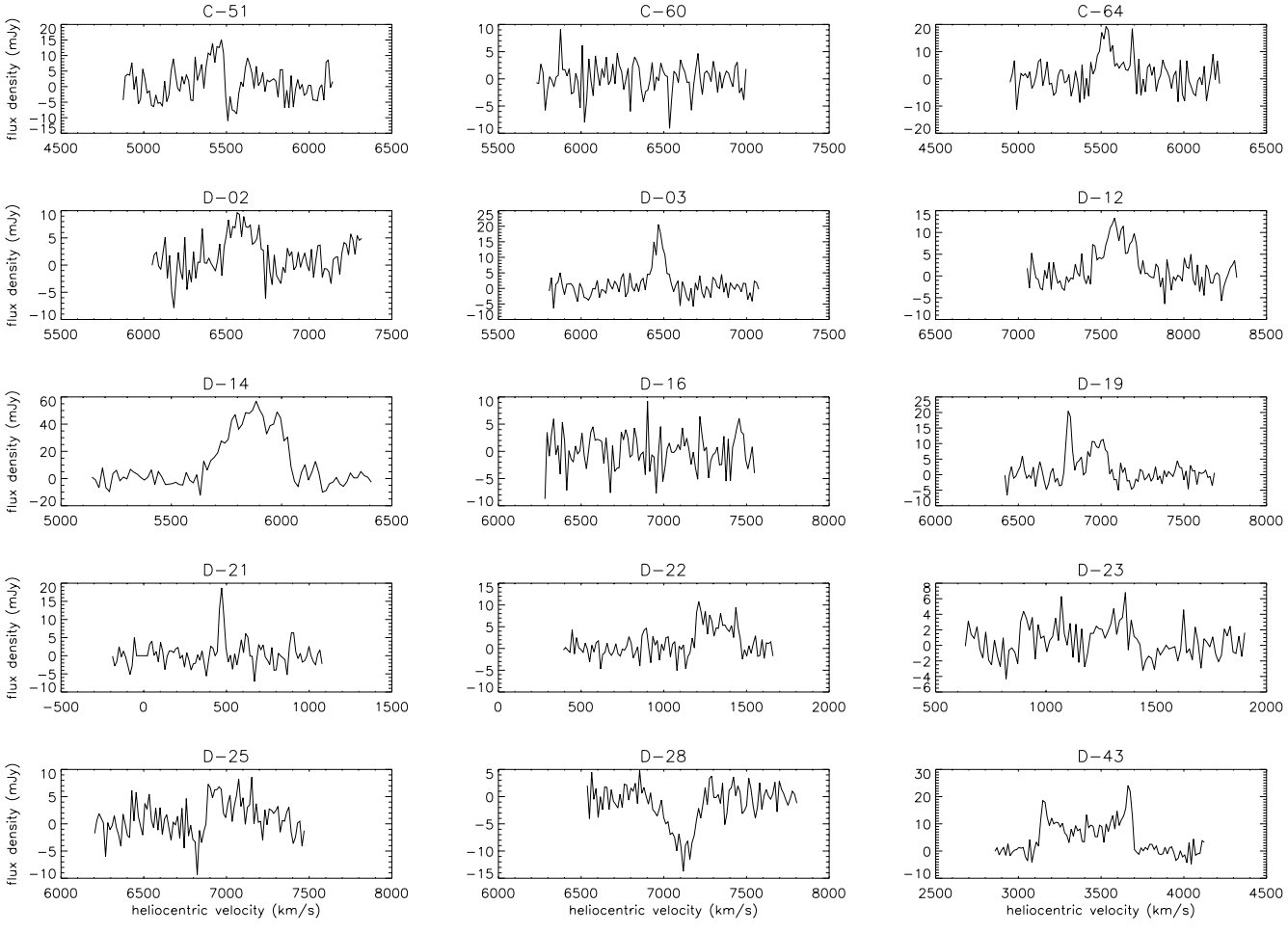

Fig. 1. c) Nançay 21-cm H I line spectra – continued

(1998). A Seyfert-type nuclear spectrum was reported in Reshetnikov & Combes (1994), though the work by Braatz et al. (1996) shows no optical emission lines. Asymmetric Hα rotation curve (Reshetnikov & Combes 1994), probably due to extended dust features. No H_2O megamaser activity was detected (Braatz et al. 1997). Not detected at Nançay (line flux <2.3 Jy km s^{-1}), while at Effelsberg a velocity of 5412 km s^{-1} was measured, 350 km s^{-1} lower than at Green Bank, and a two times larger FWHM (620 km s^{-1}). Three Arecibo detections (see Table 3) indicate a mean systemic velocity of 5486 km s^{-1}, a FWHM of 450 km s^{-1} (consistent with the optical velocity of 5505 ± 94 km s^{-1}) and a line flux of 2.5 Jy km s^{-1}. There appear to be no objects that could cause confusion within the Arecibo beam. One other galaxy was found within the Nançay search area: 16.2 mag object Cf11 (Corbelli et al. 1991), of unknown redshift. Also within the Nançay search area, at 6.′3 distance from C–26, lies the centre of group LGG 158 (Garcia 1993) in the Cancer II group, of unknown redshift. Ten galaxies are listed within the Green Bank HPBW in the NED database −8 with known redshifts, of which 2 with a redshift within 500 km s^{-1} of the PRC object: NGC 2562 (4999 km s^{-1}) and CGCG 119–061 (5180 km s^{-1}); neither was detected in H I, with published upper limits of 0.53 and 0.8 Jy km s^{-1}, respectively (see Huchtmeier & Richter 1989).

C–28 = NGC 2748. (E,G,J,N,W) Exhibits a faint structure perpendicular to the stellar disc, and appears to be a spiral galaxy surrounded by a polar ring. It may be in the process of forming a ring through accretion (Reshetnikov & Combes 1994). Flat Hα major axis rotation curve, H II-type nuclear spectrum (Reshetnikov & Combes 1994; Ho et al. 1997). Its optical kinematics were studied by Hagen-Thorn et al. (1996) and Courteau (1997). Deep r-band CCD surface photometry: see Courteau (1996) and Héraudeau & Simien (1996). Radial luminosity profile fit shows no evidence for a bulge (Baggett et al. 1998). The only possible other galaxy within the Nançay search area might the 16.9 mag object IRAS F09075+7631, of unknown redshift, at a distance of 10′. The FWHM of the Nançay profile (313 km s^{-1}) is consistent with the 5 other literature values (see Table 3), and much broader than the 140 km s^{-1} measured at Effelsberg.

C–30 = UGC 5101. (E,N) Shows an inner disc-like extension along the minor axis. Multicolor surface photometry: Reshetnikov et al. (1998) Ultraluminous IRAS galaxy (e.g., Sanders et al. 1988), with LINER/Seyfert spectrum (Kim et al. 1995; Veilleux et al. 1995; Goncalves et al. 1999) and OH line megamaser (Henkel 1990; Martin et al. 1989). Long-slit Hα spectrum: see Reshetnikov & Combes (1994). The Nançay profile shows a 152 $\mathrm{km\,s^{-1}}$ wide *absorption* profile centered on 12053 $\mathrm{km\,s^{-1}}$, within the $\pm$214 $\mathrm{km\,s^{-1}}$ error on the 134 $\mathrm{km\,s^{-1}}$ higher optical redshift. The profile could be an off-band detection, as the continuum flux density of the PRC object at 20 cm, 158 mJy (White & Becker 1992), seems too feeble for pronounced self-absorption. The Effelsberg observations did not cover this high velocity range. Optical imaging: see Smith et al. (1996), near-infrared imaging: see Majewski (1993), radio continuum imaging: see Crawford et al. (1996). No other galaxies were found within the Nançay search area.

C–32 = IC 575. (E,N) Has an underlying elliptical-like luminosity profile, with strong dust lanes along the major axis and a ringlike disc. Photo: see Arp (1966), surface photometry: PRC, V-band CCD image: see Mollenhoff et al. (1992), whose VLA continuum images show a compact radio core coinciding with the optical intensity peak. Detected by us at Effelsberg, but not at Nançay; no other published H I detection exists. Three other objects were found within the Nançay search area: (1.) VV 111a/b, a galaxy pair of unknown brightness and redshift, at 1.′4 distance (2.) MCG -01-25-057, a 17 mag object of unknown redshift, at 2.′3 distance, and (3.) IC 0574, a 15 mag early-type disc galaxy (SA0$^-$:), at 6.′2 distance.

C–33 = ESO 500–G41. (E,N) Shows spiral structure, unlike most other candidates, and was classified as (R)SA(r)ab in Buta (1995), with an inner and an outer ring of 0.′6 and 1.′3 diameter, respectively. The absorption line seen in the Nançay spectrum must be due to the Off-position detection of another object, centered at a velocity of 3755 $\mathrm{km\,s^{-1}}$ with profile widths $\Delta V_{50} = 61$ and $\Delta V_{20} = 233$ $\mathrm{km\,s^{-1}}$, as the Effelsberg profile shows only H I emission. The Nançay emission line detection of C–33 may in principle be confused by this Off-band detection, but the Nançay and Effelsberg central emission line velocities correspond to within 10 $\mathrm{km\,s^{-1}}$. No other galaxies were found within the Nançay search area.

C–34 = NGC 3384. (A,G,J,N) Classified as $\mathrm{SB0_1}$ in the RSA, it shows a disc-like component in the inner regions along the minor axis (Davoust et al. 1984). It has a disc-to-bulge luminosity ratio of 0.9, a disc scalelength of 2.7 kpc (Fisher et al. 1996; Baggett et al. 1998) and a central stellar velocity dispersion of 150 $\mathrm{km\,s^{-1}}$ (Fisher et al. 1996; Prugniel & Simien 1996). Near-infrared photometry: see Jungwiert et al. (1997). Optical spectra: stellar line strengths and their gradients were measured by Fisher et al. (1996); no emission lines are visible in the spectra of Ho et al. (1995, 1997). No stellar counter-rotation was found by Kuijken et al. (1996), only a suggestion of independent kinematical components like nuclear discs and bars. Member of the LGG 217, or Messier 96 (Leo I), group (Garcia 1993). Part of a second, stronger, line profile is seen at the high end of the Nançay band (at $1150 - 1400$ $\mathrm{km\,s^{-1}}$), which is undoubtedly due to NGC 3389, a 12.4 mag Sc spiral at the edge of the Nançay beam (2.′8 E and 5.′7 S of C–34) at an H I redshift of 1298 $\mathrm{km\,s^{-1}}$ with a FWHM of about 245 $\mathrm{km\,s^{-1}}$ (Helou et al. 1981; Staveley-Smith & Davies 1988) and a line flux of about 26 Jy $\mathrm{km\,s^{-1}}$. The PRC object was detected at Nançay (line flux 1.5 Jy $\mathrm{km\,s^{-1}}$), but not at Arecibo – the best published Arecibo upper limit is 0.62 Jy $\mathrm{km\,s^{-1}}$ (see Table 3). The well-established optical redshift of the PRC object, 735 $\pm$ 36 $\mathrm{km\,s^{-1}}$, is 170 $\mathrm{km\,s^{-1}}$ lower than the Nançay value, 903 $\mathrm{km\,s^{-1}}$, and the H I profile is quite narrow, $\Delta V_{20} = 93$ $\mathrm{km\,s^{-1}}$. Given this descrepancy, the non-detection at Arecibo and the lack of confusing galaxies in the neighbourhood, we may have detected a tail or bridge of H I far from the galaxy's center due to interaction with its nearby companion NGC 3379, a 10.2 mag elliptical at a redshift of 888 $\mathrm{km\,s^{-1}}$.

C–35 = NGC 3414. (A,E,G,N) Has unusual isophotes, considered to be a box or X-galaxy by Whitmore & Bell (1988), and faint extensions perpendicular to the major axis suggest the possibility of a ring (PRC). Has an optical LINER emission line spectrum (Ho et al. 1995, 1997) The central stellar velocity dispersion is 253 $\mathrm{km\,s^{-1}}$ (see Prugniel & Simien 1996, and references therein), and the maximum stellar rotation velocity about 55 $\mathrm{km\,s^{-1}}$ (Lake & Dressler 1986). Three other objects were found within the Nançay search area: (1.) NPM1G +28.0180 (Klemola et al. 1987), a 16.1 mag object at a redshift of 1142 $\mathrm{km\,s^{-1}}$, at 2′ distance, (3.) NGC 3418, a 14.1 mag early-type (SAB(s)0/a:) spiral with an optical redshift of 1251 $\pm$ 52 $\mathrm{km\,s^{-1}}$, at 8.′5 distance, and (3.) UGC 5958, a 15.3 mag Sbc spiral at 7.′6 distance, detected in H I at Arecibo with a line flux of about 2.6 Jy $\mathrm{km\,s^{-1}}$ at a redshift of 1182 $\mathrm{km\,s^{-1}}$ with a FWHM of 185 $\mathrm{km\,s^{-1}}$ (Bicay & Giovanelli 1986; Giovanelli et al. 1997; Schneider et al. 1986). The PRC object has a well-established optical redshift of 1445 $\pm$ 63 $\mathrm{km\,s^{-1}}$. Our Nançay and Effelsberg spectra do not even show an overlap in velocity (the measured mean velocities and ΔV_{20} widths are 1173, 325: $\mathrm{km\,s^{-1}}$ and 1526, 322 $\mathrm{km\,s^{-1}}$, respectively), and the Effelsberg integrated line flux is 2.5 times smaller than the Nançay value. The two published Arecibo profiles of the PRC object, which should be free of confusion with NGC 3418 and UGC 5958, do not have any overlap in velocity either, as their mean velocities and FWHMs are 1414, 330 $\mathrm{km\,s^{-1}}$ (Bieging & Biermann 1977) and 1592, 256 $\mathrm{km\,s^{-1}}$(DuPrie & Schneider 1996), respectively. DuPrie & Schneider actually mapped the NGC 3414

group at Arecibo and found no evidence of extended H I features within the group.

C–37 = UGC 6182. (E,G,N) One other galaxy was found near the edge of the Nançay search area: UGC 6182, a 14.7 mag spiral of unknown redshift and 1.′3 diameter, at 12.′5 distance.

C–38 = NGC 3934. (A,E,G,N) Already recognized as a PRG by Schweizer et al. (1983); CCD images (PRC) show a structure resembling two crossed discs in the inner regions, as well as extensive shells in the outer region. The galaxy was observed at Nançay as the Effelsberg profile is much stronger (15.9 vs. 5.7 Jy km s^{-1}) and wider (ΔV_{20} 317 vs. 91 km s^{-1}) than measured at Green Bank; also, the Green Bank spectrum shows only one peak, while the Effelsberg data show two. The Nançay spectrum shows 3 peaks, centered at about 3610, 3775 and 3805 km s^{-1}; at Green Bank only the middle peak was detected, while at Effelsberg both the middle and the lowest-velocity peak were seen. The Green Bank observations may well be unreliable, however, as they were plagued by solar interference, affecting the baseline. Published Arecibo detections (see Table 3) indicate detections of the middle peak only (V = 3740 km s^{-1} and ΔV_{20} = 290 km s^{-1}, I = 4.4 Jy km s^{-1}). The peaks at 3610 and 3775 km s^{-1} may well be due to confusion by 14.3 mag NGC 3933, located 2.′7 W and 2.′6 S of the PRC object, on the edge of the Nançay beam but well inside the other beams. H I spectra of NGC 3933 (see Huchtmeier & Richter 1989) show a systemic velocity of about 3731 km s^{-1} and a ΔV_{20} width of 355 km s^{-1}, measured with the 1.′9 radius Arecibo beam, and thus in principle free of confusion by C–38 at a distance of 3.′7, unless it has an H I size much larger than its optical dimensions, about 1′ diameter. The question remains why the narrow peak at 3805 km s^{-1} was observed only at Nançay; no other galaxies were found within the Nançay search area, and only one catalogued object of unknown redshift (16 mag UGC 6835) was found at the edge of the Effelsberg beam, 6.′2 from C–38.

C–39 = NGC 4174. (A,E,G,N) Very faint polar ring-like feature, CCD image: see PRC. All our H I survey profiles are likely to be confused, as it is in a compact group of galaxies, HCG 61 (Hickson 1982). The Green Bank and Effelsberg line fluxes are comparable (average 11 Jy km s^{-1}) and 2.3 times higher than measured at Nançay, while the Effelsberg profile width (262 km s^{-1}) is 1.8 times narrower than the others. CCD imaging (broad-band and Hα: see Hickson et al. (1988), Mendes de Oliveira & Hickson (1994), Vilchez & Iglesias-Paramo (1998a, 1998b). The optical redshift of the PRC object is 4010 ± 73 km s^{-1}. Several other objects were found within the Nançay search area: (1.) NGC 4175, a 14.2 mag Sbc spiral with an optical redshift of 4001 ± 43 km s^{-1}, at 1.′5 distance, (2.) NGC 4169, a 13.1 mag early-type (S0a) galaxy with an optical redshift of 3783 ± 28 km s^{-1}, at 2.′4 distance, (3.) NGC 4170, a 13.6 mag Sdm spiral at the much lower redshift of (4.) 1127 km s^{-1}, at 3.′4 distance, and (5.) three 17–18 mag galaxies, Nos. 101–103 from Kent et al. (1993), of unknown redshift, at about 5.′5 distance. Even the published Arecibo spectrum of Sulentic & Arp (1983) is bound to be confused - note its width of 547 km s^{-1} (Table 3).

C–41 = IC 3370. (G,N) Though generally considered a box-shaped elliptical, with a prominent dust lane in its inner regions, there is evidence for cylindrical rotation and X-shaped isophotes (Jarvis 1987; Goudfrooij 1994a, 1994b; Keel & Wu 1995; Penereiro et al. 1994). Two possible nuclei in addition to the primary one were identified by Forbes et al. (1994). The central stellar velocity dispersion is 202 km s^{-1} (see Prugniel & Simien 1996), and the maximum stellar rotation velocity about 95 km s^{-1} (Carollo et al. 1993; Jarvis 1987). Detected at Green Bank, but not at Nançay (with a higher rms noise). No other object was found within the Nançay search area.

C–44 = NGC 5103 (E,G) This object has an optical redshift of 1283 ± 50 km s^{-1}. Our Effelsberg and Green Bank profiles show the same central velocity (1289 km s^{-1}) and ΔV_{20} width (141 km s^{-1}), though the Effelsberg flux (6.8 Jy km s^{-1}) is almost two times larger. Of the 3 other published Green Bank profiles (see Table 3), one has a mean velocity of 1289 km s^{-1}, while the two others are centered on 1225 km s^{-1}, with a line flux of 10.5 Jy km s^{-1}, 3 times that of the other spectrum.

C–46 = ESO 576–G69. (E,G,N) Galaxy wrapped by a series of optical arcs, and with a long tidal tail. CCD imaging: see Giraud (1986). Also identified as possible PRG in Buta (1995). Not detected at Nançay (line flux <2.3 Jy km s^{-1}), while the Effelsberg profile is 4.5 times broader (464 km s^{-1}) than the Green Bank profile, and has a 400 km s^{-1} lower central velocity. The strong and broad Nançay detection by Boissé et al. (1988) is incompatible with any of our survey data (see Table 3), and may be spurious. Two other galaxies were found within the Nançay search area: (1.) ESO 576–G070, a 14.6 mag lenticular of unknown redshift and a diameter of 1.′3, at 5′ distance, and (2.) IRAS F13274–2051, a 15.7 mag object of unknown redshift, at 11.′6 distance.

C–49 = NGC 6028. (A,E,N) The nearest and brightest outer ringed, Hoag-type galaxy. Images and surface photometry, as well as a discussion of the nature of the object: see Schweizer (1987), Wakamatsu (1990) and Gavazzi et al. (1995). No other galaxies were found within the Nançay search area.

C–50 = UGC 10205. (E,G,N) Looks like a normal SO/a-Sa type galaxy in many respects, but its edge-on absorption "disc" (Gavazzi & Randone 1994) shows evidence for a brightness bump in the light profile and a warp (PRC), and deep exposures indicate diffuse debris and shell structure in the outer regions (Rubin 1987, PRC). Long-slit Hα spectra show 3 gas kinematic components structures along the major axis, one of which is in counterrotation (Rubin et al. 1985; Vega et al. 1997).

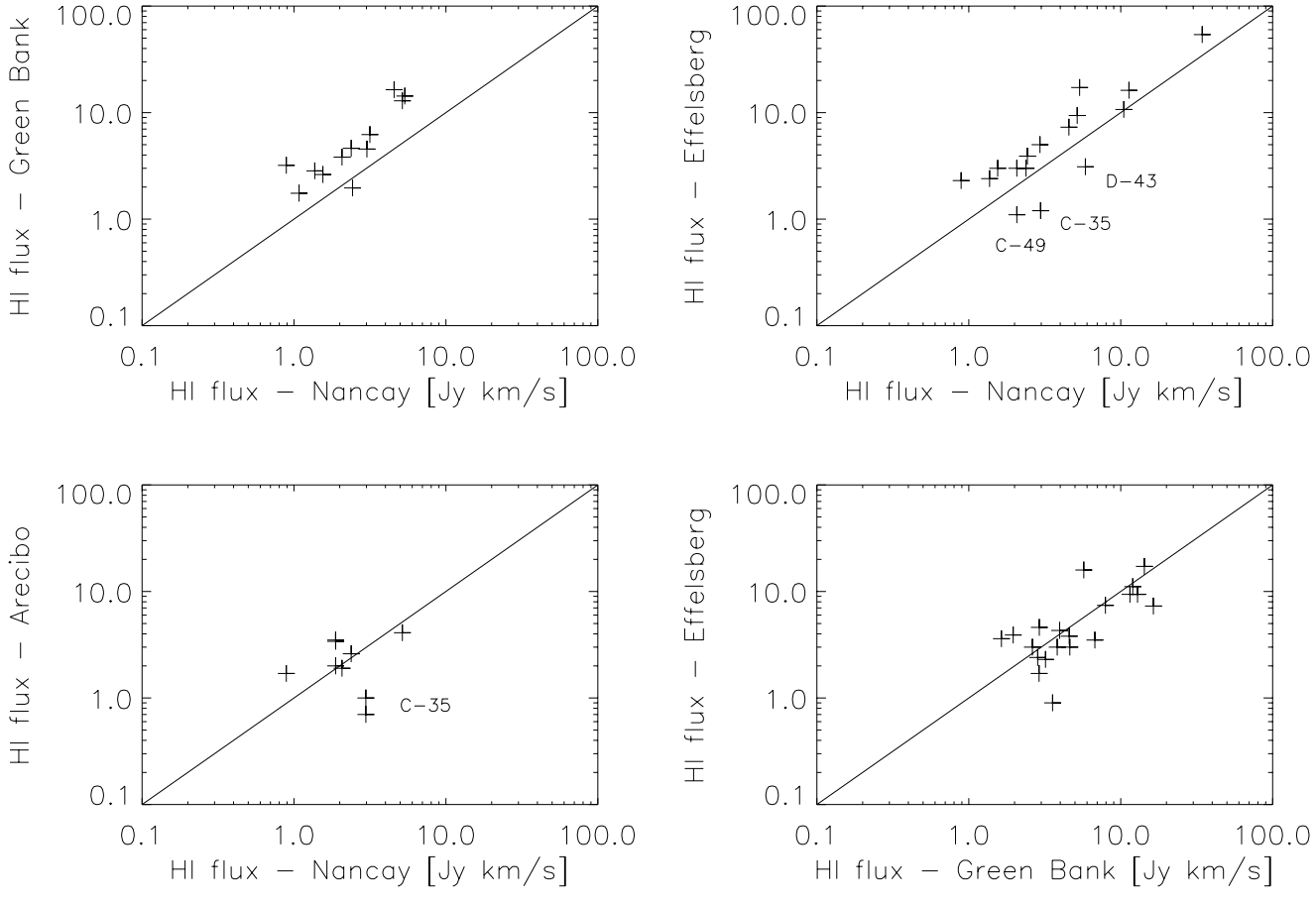

Fig. 2. A comparison of integrated H I line fluxes, on a logarithmic scale, from the present survey at Nançay, Green Bank and Effelsberg, as well as from other published sources for the Arecibo observations. To guide the eye, a diagonal solid line with a slope of 1 was plotted in each pannel; these lines are not fits to the data. **a)** Nançay vs. Green Bank, **b)** Nançay vs. Effelsberg, **c)** Nançay vs. Arecibo (literature values), and **d)** Green Bank vs. Effelsberg

Low-resolution near-infrared mapping: see Giovanardi & Hunt (1996). Its main peculiarities were modeled by Reshetnikov & Evstigneeva (1999) as the early stage in the capture and tidal disruption of a small type E/S0 companion by the massive central galaxy. Compared to the Nançay and Effelsberg results, the Green Bank central velocity is 213 $\mathrm{km\,s^{-1}}$ higher and its 163 $\mathrm{km\,s^{-1}}$ FWHM is much narrower than the 560 $\mathrm{km\,s^{-1}}$ measured elsewehere, though the line fluxes are similar. The only possible companion, at the edge of the Nançay search area (12′.7 distance), might be IRAS F16036+3019, of unknown redshift.

C–51 = NGC 6285+6286. (E,G,N) Clear tidal interaction between this close pair (1′.5 separation), and both have debris highly inclined to their central planes. More southern NGC 6286 is the more obvious PRG candidate (according to PRC), while Reshetnikov & Combes (1994) and Reshetnikov et al. (1996) interpret it as a *spiral* (as opposed to the regular, S0-type, central PRG discs) with a ring of a size comparable to that of the galaxy in an early stage of formation, rotating in an orthogonal plane, accompanied by accretion onto NGC 6285. Deep CCD images show filaments between the systems (see PRC). NGC 6285 Hα velocity field and surface photometry: see Reshetnikov et al. (1993b, 1995, 1996). Near-infrared imaging shows the mildly disturbed morphology of NGC 6286, whose major axis Hα rotation curve looks regular (Smith et al. 1996). Near-infrared spectra: Smith et al. (1996), Goldader et al. 1997a); resulting starburst model: see Goldader et al. (1997b). Optical spectra show that NGC 6285 has an H II-type spectrum and a complex Hα velocity field, while NGC 6286 is a LINER (Carrasco et al. 1997; Veilleux et al. 1995; Kim et al. 1995). One other galaxy was found in the Nançay search area: UGC 10646, a 14.8 mag elliptical of unknown redshift and 1′.3 diameter, at 12′.2 distance.

C–60 = ESO 464–G31. (E,G,N) Disturbed system, appears to consist of two nearly perpendicular edge-on components, of which one is associated with faint,

extended debris. Its optical spectrum shows emission lines, but could not be classified as either Seyfert or LINER by Maia et al. (1996). Divided into two objects of magnitudes of 15.02 and 15.64 by the automated surface photometry of the ESO-LV catalog (Lauberts & Valentijn 1989). Listed as galaxy pair AM 2115–273 in Arp & Madore (1987). No other galaxy was found in the Nançay search area.

C–64 = ESO 343–IG13. (G,N) CCD imaging (No. 57 in van den Broek et al. 1991) show it to be a close, interacting IRAS galaxy pair. Both members have an H II-type spectrum (van den Broek et al. 1991; Kim et al. 1995; Veilleux et al. 1995; Sekiguchi & Wolstencroft 1993). No OH megamaser emission was found by Staveley-Smith et al. (1992). VLA 6 and 20 cm continuum imaging: see van Driel et al. (1991). One other galaxy was found in the Nançay search area, of unknown redshift: ESO 343−G012, a 16.4 mag spiral of 1.′5 diameter, at 8.′1 distance.

Systems possibly related to PRGs

D–02 = NGC 235. (E,G,N) This galaxy is member of an optical pair (CCD image: see Keel 1996) and is sometimes listed as having triple/multiple components. Optical debris connects it to its partner, NGC 232, with which the IRAS detection is associated. NGC 235a was classified as (R′)SAB(s)a in Buta (1995), with an outer ring of 0.′56 diameter. Hubble Space Telescope imaging of the inner regions: Malkan et al. (1998). Classified as a Seyfert by Maia et al. (1987); no optical emission lines were found by Braatz et al. (1997). No H_2O megamaser activity was detected (Braatz et al. 1996). One other galaxy was found in the Nançay search area: NGC 232, a 14.4 mag SB(r)a? pec type spiral at only 2′ distance with a mean optical redshift (LEDA) of 6733 ± 53 km s^{-1}, 69 km s^{-1} higher than the optical redshift of the PRC object (6664 ± 48). The only published H I observation of NGC 232 was obtained with Nançay: at 1.′5 E and 2.′5 S of NGC 235, i.e. well within the Nançay HPBW, Martin et al. (1991) detected H I with a line flux of 1.66 Jy km s^{-1}, at $V_{\rm hel}$ = 6675 km s^{-1} and with ΔV_{20} = 411 km s^{-1}.

D–03 = ESO 474–IG28. (E,G,N) Photograph: see Johansson (1988). Optical spectroscopy (Johansson 1988) shows an H II-type starburst spectrum, and Coziol et al. (1994) identified it as an UV-bright galaxy. One other object was found at the edge of the Nançay search area: MCG +04-03-007, a galaxy pair at 13.′9 distance, at a redshift of 16,000 km s^{-1}, far outside our velocity range.

D–04 = ESO 296–G11 (G) Photometric and spectroscopic observations (Aguero et al. 1999) of this system, a.k.a. the Boomerang, show that it consists of two advanced late-type galaxies with similar general properties, which form a triple system together with a small nearby galaxy. Optical redshifts are 5267 ± 53 (NW object) and 5052 ± 35 km s^{-1} (SE object), respectively. The integrated B magnitude of the pair is listed as 14.41, and that of the SE object as 17. Of the two Green Bank detections, the weaker one, centered at 5593 km s^{-1}, is marginal, and the stronger is centered at 5192 km s^{-1}. No catalogued confusing objects were found within the Green Bank beam.

D–12 = UGC 4892. (E,N) Possibly in the process of forming a ring through accretion (Reshetnikov & Combes 1994). Has a Seyfert/LINER-type nuclear spectrum, the suspected ring shows a linear Hα rotation curve (Reshetnikov & Combes 1994). Three other galaxies were found in the Nançay search area, of which the first pair might be a source of H I confusion: (1.) MCG +08-17-066, a 17 mag 0.′3 diameter superimposed galaxy pair at 6.′9 distance, at $V_{\rm opt}$=7806 ± 32 km s^{-1} (Fisher et al. 1995), only 28 km s^{-1} higher than the Nançay profile central velocity, and (2.) MCG +08-17-067, a 16.9 mag 0.′4 diameter object at 7.′7 distance of unknown redshift.

D–14 = UGC 5485. (E,N) May be similar to an X- or box-shaped galaxy (PRC). Two other galaxies were found in the Nançay search area: MCG +11-13-004 and MCG +11-13-005. Both are 18$^{\rm th}$ mag objects of 0.′2 average diameter without known redshifts, not likely to confuse our H I emission line search out to a redshift of 10000 km s^{-1}.

D–16 = NGC 3406. (E,N) Not detected at Nançay and Effelsberg (line flux <2.4 Jy km s^{-1}). Pair of early-type galaxies, separation 20″, optical radial velocities are 7473 and 7138 km s^{-1}, respectively (Davoust & Considère 1995). The central stellar velocity dispersion is 321 km s^{-1} (White et al. 1983). Not detected in radio continuum (Cordey 1986). Listed as pair in the NED database: a 14.1 mag E-type of 1.′1 diameter at redshift 7473 ± 10 km s^{-1}, and a 14.9 mag S0 of 0.′6 diameter at 7138 ± 50 km s^{-1}. One other galaxy was found in the Nançay search area: NGC 3410, at 1.′9 distance, a 15.1 mag probable spiral with two highly discrepant published optical redshifts, 7105 (White et al. 1983) and 8292 km s^{-1} (Huchra et al. 1983).

D–19 = NGC 3808b = UGC 6643. (A,G,N) Northern member of a close interacting pair with luminous bridge and short tails, see the CCD images by Gavazzi & Randone (1994), Laurikainen et al. (1998) and Reshetnikov et al. (1996); Hα imaging by Gavazzi et al. (1998); near-infrared photometry by Gavazzi et al (1996b) and Grauer et al. (1998). Considered (Reshetnikov & Combes 1994; Reshetnikov et al. 1996) a galaxy in the process of forming a ring rotating around the major axis of the galaxy through accretion, with a size comparable to that of the galaxy. Very peculiar Hα kinematics, with a noticeable offset between the photometric and kinematic centres; the ring (in formation) has a nearly straight Hα rotation curve (Reshetnikov & Combes 1994; Reshetnikov et al. 1996). Has a nuclear spectrum on the boundary of AGN and H II-type spectra (Reshetnikov & Combes 1994). Listed as pair, with a 1.′1 separation: NGC 3808a, a 14.1 mag SAB(rs)c:pec object of 1.′7 diameter at a

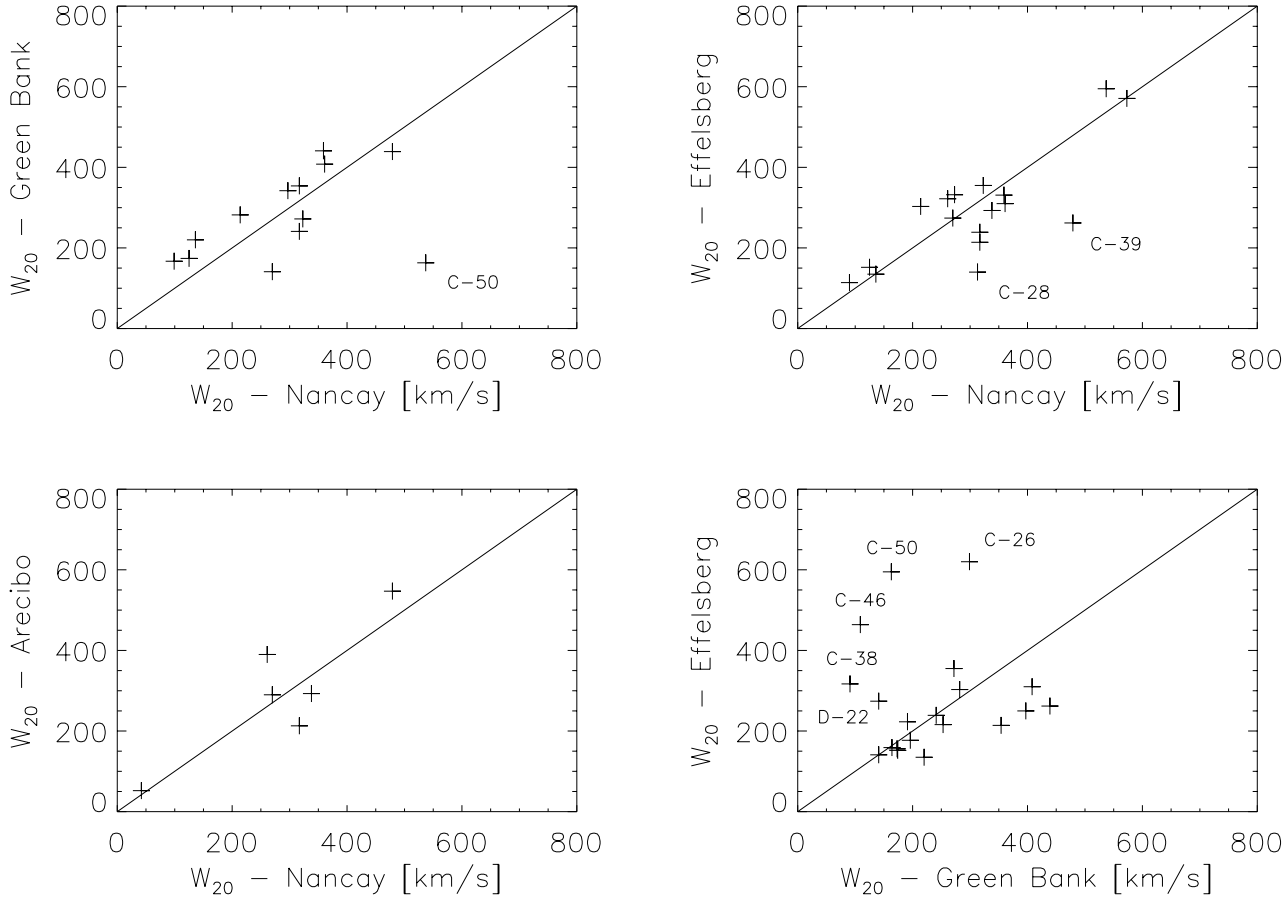

Fig. 3. A comparison of H I line widths W_{20} from the present survey at Nançay, Green Bank and Effelsberg, as well as from other published sources for the Arecibo observations. To guide the eye, a diagonal solid line with a slope of 1 was plotted in each pannel; these lines are not fits to the data. **a)** Nançay vs. Green Bank, **b)** Nançay vs. Effelsberg, **c)** Nançay vs. Arecibo (literature values), and **d)** Green Bank vs. Effelsberg

mean optical redshift of 7050 ± 38 $\mathrm{km\,s^{-1}}$ (LEDA), and NGC 3808b (the PRC object), a 15 mag I0? pec object of 0.′5 diameter, at 7189 ± 55 $\mathrm{km\,s^{-1}}$ (LEDA). No other objects were found in the Nançay search area.

D–21 = UGC 7636. (A,E,N,W) *V*-shaped low-surface brightness galaxy located 5.′6 to the SE of the giant Virgo Cluster elliptical NGC 4472, with which it is in tidal interaction; see the review paper on dwarf ellipticals by Ferguson & Binggeli (1994). CCD photometry: see McNamara et al. (1994) and Patterson & Thuan (1996). The Nançay and Effelsberg detection are associated with an H I cloud unrelated to the PRC object: an Arecibo observation (Kumar & Thonnard 1983) with a 3.′8 round beam pointed towards the NW of D–21 showed a narrow emission feature, like our data. An H I profile (Patterson & Thuan 1992) taken with the large beam of the Green Bank 43-m. telescope shows an additional, underlying broad component. Subsequent WSRT H I line imaging has shown the existence of an H I cloud halfway between both galaxies (Henning et al. 1993; Sancisi et al. 1987). The mean optical redshifts of the bright elliptical and D–21 listed in the LEDA database are, respectively, 982 ± 49 and 276 ± 60 $\mathrm{km\,s^{-1}}$ (see Binggeli et al. 1993). The redshift of the H I cloud is 466 $\mathrm{km\,s^{-1}}$, its centre position is located 2.′2 to the SW of the centre of D–21 (i.e., well within the Nançay HPBW) and its line flux is 0.49 Jy $\mathrm{km\,s^{-1}}$. WSRT and Arecibo observations (see Sancisi et al. 1987) place an upper limit of 2.25 Jy $\mathrm{km\,s^{-1}}$ for the integrated H I line flux of D–21, which we have assumed to be at the distance of the Virgo Cluster, 13.5 Mpc. Optical surface photometry: see Binggeli & Cameron (1993) and Gallagher & Hunter (1989), near-infrared surface photometry: see James (1991), where the object is referred to as VCC 1249. No other galaxy was found within the Nançay search area and velocity range.

D–22 = NGC 4643. (A,E,G,N) Very faint, disclike feature aligned with the major axis of this otherwise normal-looking barred spiral, extending to about three times the optical radius of the inner galaxy. Has a

Table 3. Other published H I data for the combined polar ring galaxy H I sample

PRC No.	Tel. Code	$V_{\rm HI}$ [km s^{-1}]	$\int S\,{\rm d}V$ [Jy km s^{-1}]	ΔV_{20} [km s^{-1}]	ΔV_{50} [km s^{-1}]	Ref.	PRC No	Tel. Code	$V_{\rm HI}$ [km s^{-1}]	$\int S\,{\rm d}V$ [Jy km s^{-1}]	ΔV_{20} [km s^{-1}]	ΔV_{50} [km s^{-1}]	Ref.
A–01	V	5528	1.1	374	411	vG87	A-03	G	930	15.3			K77
	V		2.9	385		C95		W	870	30.9		282	S80
A–02	V	4604	3.7		328	vG87	A-05	V	2910	16.0	243	231	vG87
A–03	N	868	28.5	345	260	B72		AT	2905	23.1	240	221	A97
	N	880	45.0	390		B79		P	2910		220		B97
	E	870	32.3	307	280	Bi78	A-06	W	5407	3.6	443	385	S84
	G43	875	24.6	342	298	G75		V		4.3	385		C95
B–01	P	1763	10.9	175	227	*	B–17	A	1258	12.1	218		GG81
B–03	A		<0.56			GH89		A	1255	10.5	204	171	TM81
	V		<0.55			vG87		N	1238	13.2	314	199	L73
B–11	G	2764	11.2			B87		V	1255	12.5			C95
B–16	N	2859	2.6	365	254	T98		W	1255	8.6			Ba78
	V		6.5	400		C95	B–19	P	5181	2.4	164	235	*
B–17	A	1257	9.0			DR78	B–21	P	3184	14.4	217	295	*
C–06	A		<1.0			G86	C–29	E	2619	7.7	502	432	H94
	A		<3.0			KS80	C–34	A		<0.62			BB77
C–11	IAR	370	35.1	103	80	BM85		A		<0.8			G83
	P	387	26.0			B88	C–35	A	1414	1.0	390	330	BB77
	G43	404	32.4			FT81		A	1592	0.72		256	DS96
	P	387	38.0	116		R82	C–37	G	1226	13.3	138	97	HG91
C–13	N	855	227.8	400	332	B80	C–38	A	3779				B85d
	G	851	129.2			DS83		A	3699	4.38	290	251	HR89
	G43	851	150.9			DS83	C–39	A	3922	4.1	547		SA83
	G	856	177.7	332	309	FT81	C–42	P	3289	15.6	403	356	A89
	G	852	150.3			R80	C–44	G	1289	3.2	140	112	HG91
	A	848	>52.0	324	306	S86		G	1225	10.5			RH91
	G	851	154.6	325		TC88		G	1225	10.4	230	130	HR89
	W	846	135	322	304	vD95	C–45	P	559	52.0	551	528	GW76
C–14	P		<10.4			H81		R	567	231	231		G80
C–18	N	1789	0.61	147	54	F90	C–46	N	5366	17.5	740	585	B88
	N	1744	0.17	118	98	MG98	C–49	A	4475	1.9	293	276	G81
C–24	A	6421	2.58	213	146	BG87	C–50	N	6556	2.0	564	548	T98
C–26	A	5480	1.3			B85c	C–51	G		<4.5			HR89
	A	5496	2.32	493	436	BG86	C–69	A	2083	10.0	193	155	GH93
	A	5482	2.83		462	H97		A	2081	12.8	203	158	TM81
C–27	A	1969	6.6	196	169	HG84		A	2083	12.3	223		GG81
C–28	G	1476	33.5	319		AW86		A	2081	10.0	200		H81
	J	1473	31.1	318	287	D80		A	2083	10.0		159	KS80
	W	1476	29.4	319		K96		B	2081	14.1			H98
	G	1466	7.0		294	M94		E	2083	2.5		146	H95
	E	1488	42.1	313		WK91		N	2093	17.4	259	187	B75
	G	1476	33.5	319		HR89		V	2081				BK88
D–15	A	993	70.5			H82	D–35	G43		<8.3			B76
	E	992	63.1	229	173	B83		N	4720	3.6	470	330	D90
	G	989	113.2	200		H82		V		4.0			H94
	G	970	59.5	244	179	PS74	D–43	N	3455	4.1	575	565	T98
	G	992	63.1	229	173	HR89	D–44	A	2174	8.8			DS83
	N	994	62.9	250	183	B70		A	2178	5.4		160	G87
	W	987	62.3	258	176	M95		A	2281	18.0	450	388	L93
D–16	G		<3			DS83		A	2267		481		M82
D–19	A	7078	3.4	290		C83		A	2255	18.2	429		TW82
	A	7080	2.0	293		SA83		A	2174	8.8			DS83
	A	7067	3.5	352	289	B85c		G	2178	19.0			DS83
	A	7076	3.5		269	H97		G	2162	25.4	217	158	DR78
D–21	A,W		<2.2			S.3.2		G	2260	31.4	288	140	PS74
D–22	A		1.66			KS79		G	2162				RD76
D–23	G		<3.5			RH87		G	2193	23.2	220	135	S78
D–25	A		<1.8			B87		G43	2247	38.8			DS83
D–28	A	7298	−6.8	345	490	C87		J	2280	44.8			LD87
	A	7287	−4.2		173	G87		N	2230	42.9	335	135	B82
	A	7270	−5.9	570	360	B85	D–46	A	3086	4.0	274	239	L87
	A	7350	*abs.*	705	365	H83		A	3072	3.4	286	253	SK78
	V	7256	*abs.*		405	D82		G	3090	3.0	245	220	RH91

H I references and telescope codes to Table 3

A89	Aaronson et al. (1989)	AW86	Armstrong & Wootton (1986)	A97	Arnaboldi et al. (1997)
B85	Baan et al. (1985)	BM85	Bajaja & Martin (1985)	B76	Balick et al. (1976)
B72	Balkowski et al. (1972)	Ba78	Balkowski (1978)	B79	Balkowski (1979)
B97	Barnes et al. (1997)	B88	Becker et al. (1988)	BG86	Bicay & Giovanelli (1986)
BG87	Bicay & Giovanelli (1987)	Bi78	Bieging (1978)	BB77	Bieging & Biermann (1977)
B83	Bohnenstengel (1983)	B88	Boissé et al. (1988)	B85a	Bothun et al. (1985a)
B85b	Bothun et al. (1985b)	B70	Bottinelli et al. (1970)	B75	Bottinelli et al. (1975)
B80	Bottinelli et al. (1980)	B82	Bottinelli et al. (1982)	BK88	Brinks & Klein (1988)
B87	Bushouse (1987)	C87	Chamaraux et al. (1987)	C83	Chincarini et al. (1983)
C95	Cox et al. (1995)	D80	Davies (1980)	DS83	Davis & Seaquist (1983)
DR78	Dickel & Rood (1978)	DR80	Dickel & Rood (1980)	D82	Dickey (1982)
D90	Dupraz et al. (1990)	DS96	DuPrie & Schneider (1996)	FT81	Fisher & Tully (1981)
F90	Fouqué et al. (1990)	G75	Gallagher et al. (1975)	GW76	Gardner & Whiteoak (1976)
G87	Garwood et al. (1987)	G83	Giovanardi et al. (1983)	G81	Giovanelli et al. (1981)
G86	Giovanelli et al. (1986)	GH89	Giovanelli & Haynes (1989)	GH93	Giovanelli & Haynes (1993)
GG81	Gordon & Gottesman (1981)	G80	Gosachinskii et al. (1980)	H81	Hawarden et al. (1981)
H81	Haynes (1981)	HG91	Haynes & Giovanelli (1991)	H97	Haynes et al. (1997)
H98	Haynes et al. (1998)	H83	Heckman et al. (1983)	H94	Hibbard et al. (1994)
H94	Huchtmeier (1994)	HR89	Huchtmeier & Richter (1989)	H82	Hunter et al. (1982)
H95	Huchtmeier et al. (1995)	K96	Kamphuis et al. (1996)	K77	Knapp et al. (1977)
KS79	Krumm & Salpeter (1979)	KS80	Krumm & Salpeter (1980)	L73	Lauqué (1973)
L87	Lewis (1987)	LD87	Lewis & Davies (1973)	L93	Lu et al. (1993)
M94	Magri (1994)	M98	Matthews et al. (1998)	M82	Mirabel (1982)
M95	Mulder et al. (1995)	PS74	Peterson & Shostak (1974)	R82	Reif et al. (1982)
RH87	Richter & Huchtmeier (1987)	RH91	Richter & Huchtmeier (1991)	RD76	Rood & Dickel (1976)
R80	Rots (1980)	S86	Schneider et al. (1986)	S80	Shane (1980)
S84	Schechter et al. (1984)	S78	Shostak (1978)	SK78	Silvergate & Krumm (1978)
SA83	Sulentic & Arp (1983)	T98	Theureau et al. (1998)	TM81	Thuan & Martin (1981)
TW82	Thuan & Wadiak (1982)	TC88	Tifft & Cocke (1988)	vD95	van Driel et al. (1995)
vG87	van Gorkom et al. (1987)	WK91	Wunderlich & Klein (1991)	*	This paper
A	Arecibo 305-m	AT	Australia Telescope	E	Effelsberg 100-m
G	Green Bank 90-m	G43	Green Bank 43-m	IAR	I.A.R. 30-m
J	Jodrell Bank 76-m	N	Nançay 94-m equiv.	P	Parkes 64-m
R	RATAN 600	V	VLA	W	Westerbork

LINER-type optical spectrum (Boulesteix et al. 1988; Ho et al. 1997; Keel 1983). Only nuclear line emission was found in the Hα imaging by Pogge & Eskridge (1993) and only very faint, patchy circumnuclear Hα emission by Pogge (1989). Optical and near-infrared imaging (Ohta et al. 1990; Shaw et al. 1995) suggest the presence of secondary, nuclear bar. A projected maximum stellar rotation velocity of 90 $\mathrm{km\,s^{-1}}$ was derived from long-slit spectroscapy at 4 position angles by Bettoni & Galletta (1997). The Green Bank H I line profile is centered at a 250 $\mathrm{km\,s^{-1}}$ lower radial velocity than the optical redshift of the PRG and the Nançay and Effelsberg H I velocity, and the Green Bank profile width (140 $\mathrm{km\,s^{-1}}$) is two times narrower. According to Paper I, the Green Bank detection is "probably associated with a small companion galaxy of unknown redshift at 20′ distance, which nevertheless is a very gas-poor system (M_{HI}/L_B = 0.02 $M_\odot/L_{\odot,B}$)". No other galaxies were found in the Nançay search area.

D–23 = NGC 4753. (E,G,G43,N,P) Appears to be a good candidate for the formation of an X- or box-shaped galaxy by accretion (PRC); short exposures show a extensive, seemingly chaotic pattern of dust lanes (Sandage 1961), which was matched, however, by a precessing disc model (Steiman-Cameron et al. 1992). Rising Hα rotation curve, flattening out beyond 10″ radius; LINER-type nuclear spectrum (Reshetnikov & Combes 1994). Listed as member of group LGG 315 (Garcia 1993), alias the NGC 4643 and NGC 4753 groups, and group 41 from Huchra & Geller (1982). No other objects found within the Nançay search area. The Nançay and Effelsberg profile parameters are totally different; the narrow peak seen at Effelsberg does not even correspond to a peak in the broad, and weak, Nançay profile. Published H I upper limits only, the best is 3.5 Jy $\mathrm{km\,s^{-1}}$(see Table 3 and Huchtmeier & Richter 1989).

D–24 = ESO 575–G44 (E) Very close pair of galaxies of 15.06 and 13.53 mag, respectively. The optical redshift of the system (9066 ± 90 $\mathrm{km\,s^{-1}}$) is based on two measurements (Dressler 1991 and Fairall et al. 1992). This value lies outside the range of the Effelsberg H I observations, where a 390 $\mathrm{km\,s^{-1}}$ wide profile centered on 2806 $\mathrm{km\,s^{-1}}$ was detected instead. No other catalogued galaxies were found within the Effelsberg beam area. The Effelsberg detection therefore appears to be spurious.

D–25 = UGC 8387 = IC 883. (A,E,G,N) This objects shows two linear, one-sided and almost perpendicular tidal tails protruding from the centre in the optical and near-infrared (Smith et al. 1995, 1996; Stanford & Bushouse 1991, PRC). It is quite infrared luminous. Near-infrared spectra and Hα rotation curve: see Smith et al. (1996). Has a LINER optical spectrum (Kim et al. 1995; Veilleux et al. 1995). Near infrared spectrum: see Puxley (1994); near-infrared imaging:

see Zhou et al. (1993). In our survey, H I emission was observed at Green Bank only. Observations with the much smaller (3.′8 diameter) Arecibo beam show a broad, triple-peaked *absorption* feature against the continuum (Mirabel & Sanders 1988), while Bushouse (1987) measured an upper limit of 1.8 Jy km s^{-1}. No other galaxies were found within the Nançay search area.

D–28 = NGC 6240. (A,E,G,N) This galaxy is a merger product with a luminosity profile similar to that of an elliptical and it is a superliminous IRAS galaxy. In its inner parts many crossed optical loops can be seen, while the outer regions show an extensive set of shells. The H I emission line spectrum may be influenced by absorption against the strong continuum, since it is a strong radio source. CCD images: see PRC. It has a LINER optical spectrum (Goldader et al. 1997; Kim et al. 1995; Rieke et al. 1985; Veilleux et al. 1995); stellar kinematics: see Lester (1994) The object contains a strong continuum source (650 mJy at 21 cm), and thus care has to be taken in accurately determining the radio telescope's passband in both polarisations used; we did this at Nançay using a strong quasar. An *absorption* profile was detected at Nançay as well as in several Arecibo and VLA studies (see Table 3): only the Arecibo profile of Garwood et al. (1987) has a FWHM (173 km s^{-1}) comparable to our Nançay measurement, the others are considerably broader (average 405 km s^{-1}). The OH lines also show an absorption profile (Baan et al. 1985, 1992). No H_2O megamaser activity was detected (Braatz et al. 1997). Near-infrared imaging and spectrum: see Doyon et al. (1994), Rieke et al. (1985), Zhou et al. (1993). No other galaxies were found within the Nançay search area.

D–43 = ESO 510–G13. (E,G,N) Boxy system with a very thin optical disc and a dust lane along its minor axis. It was separated as two sources by the automatic ESO-LV surface photometry software. Other published Nançay detection: see Theureau et al. (1998). No other galaxies were found within the Nançay search area.

3.3. Results – comparison with the Green Bank and Effelsberg survey data and other published data

Basic H I line data obtained for our PRG survey at Green Bank, Effelsberg and Nançay are given in Table 2 for all 74 galaxies of the combined PRG H I sample. The Green Bank and Effelsberg data were taken straight from Papers I and II, respectively. The velocity resolution used at Nançay to determine the H I line parameters or upper limits is 15.8 km s^{-1} for the objects with previously known redshift and 19.0 km s^{-1} for the others.

The estimated upper limits to the integrated H I line fluxes listed in Table 2 are 3σ values for an assumed 250 km s^{-1} wide flat-topped profile; the double upper limits listed for objects without previously known redshift are for the low (340 − 5207 km s^{-1}) and high (5140 − 10007 km s^{-1}) Nançay velocity search ranges, respectively.

Most PRG objects observed are rather faint in H I, as is obvious from the signal-to-noise ratio of many of the H I profiles obtained with any of the three telescopes used for our survey. The average integrated line flux of the galaxies detected at Nançay, and plotted in Fig. 2, is only 1.7 Jy km s^{-1}. This often makes it difficult to determine really accurate profile parameters from a spectrum measured with any single telescope. We will therefore have to rely on a comparison of all available profiles per galaxy in order to derive the most reliable H I parameters possible, which can then be used to calculate derived quantities - these data will be presented and analysed in the next paper in these series (van Driel et al., in preparation).

A potentially important factor in the comparison of profiles of the same object is the significant difference in beam size for the telescopes used: 21′ round at Green Bank, 12′ round at Effelsberg, and 4′ × 22′ ($\Delta\alpha \times \Delta\delta$) at Nançay for $\delta \leq 30°$. A larger beam size may in principle lead to (1.) higher H I masses measured for galaxies with extended H I distributions, and (2.) a higher chance of confusion by other galaxies in the beam area, as detailed in the present paper (Sect. 3.2) and in the Appendix to Paper I. Another important factor is that recent projects at the three sites have shown that Nançay appears to be better protected against radio frequency interference in the 21-cm band than Green Bank and Effelsberg, avoiding spectral contamination - clear evidence of interference is shown by, e.g., the very broad Effelsberg profiles in Fig. 3.

A comparison of the integrated H I line fluxes of objects detected with different telescopes for our PRG survey, as well as between our Nançay and published Arecibo data (Fig. 2) shows a considerable scatter in all plots. On average, values measured at Nançay are generally about 2 times lower than those measured at Green Bank or at Effelsberg – of the 3 Nançay values which are about twice as *high* as the Effelsberg measurements (for C–35, C–49 and D–43) only the C–35 measurement appears to be due to confusion. On the other hand, the Nançay–Arecibo comparison shows an agreement between most measurements; confusion within the Nançay beam is the cause of the considerably higher H I flux measured at Nançay for C–35, so the Nançay and Arecibo data appear to be consistent. The comparison of our Green Bank and Effelsberg values show clustering around a ratio of 1.

Similar comparisons (Matthews et al. 1998; Matthews & van Driel 2000) of recent Nançay line fluxes of two samples of unresolved galaxies with (much) stronger H I emission, observed and reduced in exactly the same way as our PRG data, does not show a clear systematic difference with line fluxes measured at other sites (primarily Green Bank and Arecibo) by other authors, or with fluxes measured earlier at Nançay by other authors. In

conclusion, the cause of the Nançay-Green Bank/Effelsberg flux discrepancy found in our survey is not clear.

A comparison of the central H I line velocities measured with different telescopes (see Table 3) shows that most 21-cm radial velocities are rather accurate: the external error is of the order of 20 to 30 $\mathrm{km\,s^{-1}}$, compared to the 16 $\mathrm{km\,s^{-1}}$ velocity resolution of the Nançay data. Some large discrepancies are found, though, especially in the comparison between Effelsberg and Green Bank data, where 5 (out of 19) profiles of commonly observed objects have differences between 210 and 400 $\mathrm{km\,s^{-1}}$, but these seem to be due to confusion with nearby galaxies and/or radio interference signals (see the Notes in Sect. 3.2).

A comparison (Fig. 3) of H I linewidths determined at 20% of the peak intensity value, ΔV_{20}, in general shows good agreement, even without applying corrections for instrumental resolution. In the Nançay-Green Bank comparison, only one object (C–50) shows a much larger Nançay linewidth, which is consistent with the Effelsberg data. In the Nançay-Effelsberg comparison, the largest discrepancies (the broader Nançay profile of C–39) can be explained by confusion with nearby group members, while the broad width of the C–28 Nançay profile is consistent with 5 literature values. In the Green Bank-Effelsberg comparison, the most prominent exceptions are 5 galaxies (C–26, 38, 46 and 50, and D–22) for which the discrepancies appear to be due to radio interference or confusion (see Sect. 3.2). In conclusion, the discrepancies in measured line widths can be explained by radio interference or confusion with other galaxies.

Acknowledgements. We would like to thank the staff of the Nançay and ARPEGES departments of the Paris Observatory for their support with the observations and the data reduction, especially Dr. E. Gérard. We have made use of the NASA/IPAC Extragalactic Database (NED) which is operated by the Jet Propulsion Laboratory, California Institute of Technology, under contract with the U.S. National Aeronautics and Space Administration, as well as the Lyon-Meudon Extragalactic Database (LEDA) supplied by the LEDA team at the CRAL-Observatoire de Lyon (France). The Unité Scientifique Nançay of the Observatoire de Paris is associated as Unité de Service et de Recherche USR No. B704 to the French Centre National de Recherche Scientifique (CNRS). Nançay also gratefully acknowledges the financial support of the Région Centre in France.

References

Aaronson M., Bothun G.D., Cornell M.E., et al., 1989, ApJ 338, 65
Abell G.O., Corwin H.G., Olowin R.P., 1989, ApJS 70, 1
Aguereo E.L., Paolantonio S., Gunthardt G., 1998, AJ 117, 1151
Armstrong J.T., Wooten H.A., 1986, in: Light on Dark Matter, Astrophys. Sp. Sci. Lib. 124, 439
Arnaboldi M., Capacciol M., Cappellaro E., et al., 1993a, A&A 267, 21
Arnaboldi M., Barbaro G., Buson L., et al., 1993b, A&A 268, 103
Arnaboldi M., Freeman K.C., Sackett P.D., Sparke L.S., Capaccioli M., 1995, Planet. Space Sci. 43, 1377
Arnaboldi M., Oosterloo T.A., Combes F., Freeman K.C., Koribalski B., 1997, AJ 113, 585
Arp H., 1966, Atlas of Peculiar Galaxies (= ApJS 14, 1)
Arp H., Madore B., 1987, A Catalogue of Southern Peculiar Galaxies and Associations. Cambridge University Press
Baan W., Haschick A.D., Buckley D., Schmelz J.T., 1985, ApJ 293, 394
Baan W.A., Haschick A.D., Henkel C., 1992, AJ 103, 728
Baggett W.E., Baggett S.M., Anderson K.S.J., 1998, AJ 116, 1626
Bajaja E., Martin M.C., 1985, AJ 90, 1783
Balick B., Faber S.M., Gallagher J.S., 1976, ApJ 209, 710
Balkowski C., Bottinelli L., Gouguenheim L., Heidmann J., 1972, A&A 21, 303
Balkowski C., Chamaraux P., Weliachew L., 1978, A&A 69, 263
Balkowski C., 1979, A&A 78, 190
Barnes L., Staveley-Smith L., Webster R.L., Walsh W., 1997, MNRAS 288, 307
Becker R., Mebold U., Reif K., van Woeden H., 1988, A&A 203, 21
Bettoni D., Galletta G., 1997, A&AS 124, 61
Bicay M.D., Giovanelli R., 1986, AJ 91, 732
Bicay M.D., Giovanelli R., 1987, AJ 93, 1326
Bieging J.H., 1978, A&A 64, 23
Bieging J.H., Biermann P., 1977, A&A 60, 361
Binggeli B., Cameron L.M., 1993, A&AS 98, 297
Binggeli B., Popescu C.C., Tammann G.A., 1993, A&AS 98, 275
Bohnenstengel H.D., 1983, Ph.D. Thesis, Univ. Hamburg
Boissé P., Dickey J.M., Kazès I., Bergeron J., 1988, A&A 191, 193
Bothun G.D., Beers T.C., Mould J.R., Huchra J., 1985a, AJ 90, 791
Bothun G.D., Aaronson M., Schommer R., et al., 1985b, ApJS 57, 423
Bothun G.D., Beers T.C., Mould J.R., 1985d, AJ 90, 2487
Bottinelli L., Chamaraux P., Gouguenheim L., Lauqué R., 1970, A&A 6, 453
Bottinelli L., Duflot R., Gouguenheim L., Heidmann J., 1975, A&A 41, 61
Bottinelli L., Gouguenheim L., Paturel G., 1980, A&A 88, 32
Bottinelli L., Gouguenheim L., Paturel G., 1982, A&A 113, 61
Boulesteix J., Georgelin Y., Roy J.-R., 1988, A&A 200, 29
Braatz J.A., Wilson A.S., Henkel C., 1996, ApJS 106, 51
Braatz J.A., Wilson A.S., Henkel C., 1997, ApJS 110, 321
Brinks E., Klein U., 1988, MNRAS 231, 63P
Brocca C., Bettoni D., Galletta G., 1997, A&A 326, 907
Bushouse H.A., 1987, ApJ 320, 49
Buta R., Crocker D.A., 1993, AJ 106, 939
Buta R.J., 1995, ApJS 96, 39 (CSRG)
Carollo C.M., Danziger I.J., Buson L., 1993, MNRAS 265, 553
Carrasco L., Serrano A., Tovmassian H.M., et al., 1997, AJ 113, 1527
Chamaraux P., Balkowski C., Fontanelli P., 1987, A&AS 69, 263
Chincarini G.L., Giovanelli R., Haynes M.P., 1983, ApJ 269, 13

Corbelli E., Salpeter E.E., Dickey J.M., 1991, ApJ 370, 49
Cordey R.A., 1986, MNRAS 219, 577
Courteau S., 1996, ApJS 103, 363
Courteau S., 1997, AJ 114, 2402
Cox A.L., Sparke L.S., Richter O., Shaw M., 1995, in: Ninth Annual Conference on Nonlinear Astronomy, Proc. of the NY Academy of Sciences
Cox A.L., 1996, VLA H I and continuum mapping of polar ring galaxies, Ph.D. Thesis, Univ. of Wisconsin
Coziol R., Demers S., Pena M., Barneouid R., 1994, AJ 108, 405
Courteau S., 1996, ApJS 103, 363
Crawford T., Marr J., Partridge B., 1996, ApJ 460, 225
Davis L.E., Seaquist E.R., 1983, ApJS 53, 269
Davoust E., Lelièvre G., Maury A., Nieto J.-L., 1984, MNRAS 209, 503
Davoust E., Considère S., 1995, A&AS 110, 19
de Vaucouleurs G., de Vaucouleurs A., Corwin H.G., et al., 1991, Third Reference Catalog of Bright Galaxies. Springer, Heidelberg (RC3)
Dickel J.R., Rood H.J., 1978, ApJ 223, 391
Dickel J.R., Rood H.J., 1980, AJ 85, 824
Dickey J.M., 1982, ApJ 263, 87
Doyon R., Wells M., Wright G.S., et al., 1994, ApJ 437, L23
Dressler A., Schectman S.A., 1988, AJ 95, 284
Dressler A., 1991, ApJS 75, 241
Dupraz F., Casoli F., Combes F., Kazès I., 1990, A&A 228, 5
DuPrie K., Schneider S.E., 1996, AJ 112, 937
Fairall A.P., Willmer C.N.A., Calderon J.H., et al., 1992, AJ 103, 11
Ferguson H.C., Binggeli B., 1994, A&AR 6, 67
Fisher J.R., Tully R.B., 1981, ApJS 47, 139
Fisher J.R., Huchra J.P., Strauss M.A., et al., 1995, ApJS 100, 69
Fisher D., Franx M., Illingworth G., 1996, ApJ 459, 110
Forbes D.A., Thomson R.C., Groom W., Williger G.M., 1994, AJ 107, 1713
Fouqué P., Bottinelli L., Durand N., Gouguenheim L., Paturel G., 1990, A&AS 86, 473
Gallagher J.S., Faber S.M., Balick B., 1975, ApJ 202, 7
Gallagher J.S., Hunter D.A., 1989, AJ 98, 806
Galletta G., Sage L.J., Sparke L.S., 1997, MNRAS 284, 773
Garcia A.M., 1993, A&AS 100, 47
Gardner F.F., Whiteoak J.B., 1976, PASA 3, 63
Garwood R.W., Helou G., Dickey J.M., 1987, ApJ 322, 88
Gavazzi G., Garilli B., Carrasco L., Boselli A., Cruz-Gonzales I., 1994, A&AS 104, 271
Gavazzi G., Randone I., 1994, A&AS 107, 285
Gavazzi G., Boselli A., Carrasco L., 1995, A&AS 112, 257
Gavazzi G., Pierini D., Boselli A., Tuffs R., 1996a, A&AS 120, 489
Gavazzi G., Pierini D., Boselli A., Tuffs R., 1996b, A&AS 120, 521
Gavazzi G., Catinella B., Carrasco L., Boselli A., Contursi A., 1998, AJ 115, 1745
Giovanardi C., Krumm N., Salpeter E.E., 1983, AJ 88, 1719
Giovanardi C., Hunt L.K., 1996, AJ 111, 1086
Giovanelli R., Chincarini G.L., Haynes M., 1981, ApJ 247, 383
Giovanelli R., Haynes M.P., Myers S.T., Roth J., 1986, AJ 92, 250
Giovanelli R., Haynes M.P., 1989, AJ 97, 633
Giovanelli R., Haynes M.P., 1993, AJ 105, 1271
Giovanelli R., Avera E., Karachentsev I.D., 1997, AJ 114, 122
Giraud E., 1986, A&A 161, 206
Goldader J.D., Joseph R.D., Doyon R., Sander D.B., 1997a, ApJ 474, 104
Goldader J.D., Joseph R.D., Doyon R., Sander D.B., 1997b, ApJS 108, 449
Goncalves A.C., Véron-Cetty M.P., Véron P., 1999, A&AS 135, 437
Gordon D., Gottesman S.T., 1981, AJ 86, 161
Gosachinskii I.V., Grachev V.G., Ryzhkov N.F., 1980, Sov. Astron. 24, 647
Goudfrooij P., Hansen L., Jorgensen H.E., Norgaard-Nielsen H.U., 1994a, A&AS 104, 179
Goudfrooij P., Hansen L., Jorgensen H.E., et al., 1994b, A&AS 105, 341
Hagen-Thorn V.A., Reshetnikov V.P., Yakovleva V.A., 1996, Astr. Reports 40, 29
Hagen-Thorn V.A., Reshetnikov V.P., 1996, Astron. Lett. 22, 677
Hagen-Thorn V.A., Reshetnikov V.P., 1997, A&A 319, 430
Haynes M.P., 1981, AJ 86, 1126
Haynes M.P., Giovanelli R., 1991b, A&AS 77, 362
Haynes M.P., Giovanelli R., Herter T., Vogt N.P., 1997, AJ 113, 1197
Haynes M.P., Hogg D.E., Maddalena R.J., Roberts M.S., Van Zee L., 1998, AJ 115, 62
Hawarden T.G., Longmore A.J., Goss W.M., Mebold U., Tritton S.B., 1981, MNRAS 196, 175
Heckman T.M., Balick B., van Breugel W.J.M., Miley G.K., 1983, AJ 88, 583
Helou G., Giovanardi C., Salpeter E.E., Krumm N., 1981, ApJS 46, 267
Henkel C., 1990, A&A 229, 431
Henning P.A., Sancisi R., McNamara B.R., 1993, A&A 268, 536
Héraudeau Ph., Simien F., 1996, A&AS 118, 111
Hernquist L., Quinn L., 1988, ApJ 331, 682
Hibbard J.E., Guhathakurta P., van Gorkom J.H., Schweizer F., 1994, AJ 107, 67
Hickson P., 1982, ApJ 255, 382
Hickson P., Kindl E., Auman J.R., 1988, ApJS 70, 687
Ho L.C., Filippenko A.V., Sargent W.L.W., 1995, ApJS 98, 477
Ho L.C., Filippenko A.V., Sargent W.L.W., 1997, ApJS 112, 315
Hoffman G.L., Helou G., Salpeter E.E., Glosson J., Sandage A., 1987, ApJS 63, 247
Huchra J., Geller M.J., 1982, ApJ 257, 423
Huchra J., Davis M., Tonry J., Latham D., 1983, ApJS 52, 89
Huchtmeier W.K., Richter O.-G., 1989, A General Catalogue of H I Observations of Galaxies. Springer, Heidelberg
Huchtmeier W.K., 1994, A&A 286, 389
Huchtmeier W.K., Sage L.J., Henkel C., 1995, A&A 300, 675
Huchtmeier W., 1997, A&A 319, 401 (Paper II)
Hunter D.A., Gallagher J.S., Rautenkranz D., 1982, ApJS 49, 53
James P., 1991, MNRAS 250, 544
Jarvis B.J., 1987, in Structure and Dynamics of Elliptical Galaxies, IAU Symposium No. 127. Reidel, Dordrecht, p. 411

Johansson L., 1988, A&AS 73, 335
Jungwiert B., Combes F., Axon D.J., 1997, A&AS 125, 479
Kamphuis J.J., Sybring D., van Albada T.S., 1996, A&AS 116, 15
Keel W.C., 1983, ApJS 52, 229
Keel W.C., 1985, AJ 90, 2207
Keel W.C., Wu W., 1995, AJ 110, 129
Keel W.C., 1996, AJ 111, 696
Kent S.M., Ramella M., Nonino M., 1993, AJ 105, 393
Kim D.-C., Sanders D.B., Veilleux S., Mazzarella J.M., Soifer B.T., 1995, ApJS 98, 129
Klemola A.R., Jones B.F., Hanson R.B., 1987, AJ 94, 501
Knapp G.R., Gallagher J.S., Faber S.M., Balick B., 1977, AJ 82, 106
Krumm N., Salpeter E.E., 1979, ApJ 227, 776
Krumm N., Salpeter E.E., 1980, AJ 85, 1312
Kuijken K., Fisher D., Merrifield R., 1996, MNRAS 283, 543
Kumar C.K., Thonnard N., 1983, AJ 88, 260
Lauberts A., Valentijn E.A., 1989, The Surface Photometry Catalogue of the ESO-Uppsala Galaxies. ESO, Garching (ESO-LV)
Lake G., Dressler A., 1986, ApJ 310, 605
Lauqué R., 1973, A&A 23, 353
Lester D.F., Gaffney N.I., 1994, ApJ 431, L13
Lewis B.M., Davies R.D., 1973, MNRAS 165, 213
Lewis B.M., 1987, ApJS 63, 515
Loveday J., Peterson B.A., Maddox S.J., Efstathiou G., 1996, ApJS 107, 201
Lu N.Y., Hoffman G.L., Groff T., Roos T., Lamphier C., 1993, ApJS 88, 383
Magri C., 1994, AJ 108, 896
Maia M.A.G., da Costa L.N., Willmer C., Pellegrini P.S., Rité C., 1987, AJ 93, 546
Maia M.A.G., Suzuki J.A., da Costa L.N., Willmer C.N.A., Rité C., 1996, A&AS 117, 487
Majewski S.R., Hereld M., Koo D.C., Illingworth G.D., Heckman T.M., 1993, ApJ 402, 125
Makarov D.I., Karachentsev I.D., Burenkov A.N., Tyurina N.V., Korotkova G.G., 1997, Astron. Lett. 23, 638
Malkan M.A., Gorjian V., Tam R., 1998, ApJS 117, 25
Martin J.M., Bottinelli L., Dennefeld M., et al., 1989, C.R. Acad Sci. 308, 287
Martin J.M., Bottinelli L., Dennefeld M., Gouguenheim L., 1991, A&A 245, 393
Martin M.C., 1998, A&AS 131, 73
Matthews L.D., van Driel W., Gallagher J.S., 1998, AJ 116, 1169
Matthews L.D., van Driel W., 2000, A&AS (to be submitted)
McNamara B.R., Sancisi R., Henning P.A., Junior W., 1994, AJ 108, 844
Mendes de Oliveira C., Hickson P., 1994, ApJ 427, 684
Mirabel I.F., Sanders D.B., 1988, ApJ 335, 104
Mollenhoff C., Hummel E., Bender R., 1992, A&A 255, 35
Mulder P.S., van Driel W., Braine J., 1995, A&A 300, 687
Moody J., Kirshner, 1988, AJ 95, 1629
Ohta K., Hamabe M., Wakamatsu K.-I., 1990, ApJ 357, 710
Osterbrock D.E., Dehari O., 1983, ApJ 273, 478
Patterson R.J., Thuan T.X., 1992, ApJ 400, L55
Patterson R.J., Thuan T.X., 1996, ApJS 107, 103
Paturel G., Bottinelli L., Gouguenheim L., Fouqué P., 1990, Catalogue of HI Data. Obs. of Lyon and Paris-Meudon, France
Penereiro J.C., de Carvalho R.R., Djorgovski S., Thompson D., 1994, A&AS 108, 461
Peterson S.D., Shostak G.S., 1974, AJ 79, 767
Pogge R., 1989, ApJS 71, 433
Pogge R., Eskridge P.B., 1993, AJ 106, 1405
Prugniel Ph., Simien F., 1996, A&A 309, 749
Puxley P.J., Lumsden S.L., Brand P.W.J.L., Doyon R., 1994, MNRAS 270, L7
Reif K., Mebold U., Goss W.M., van Woerden H., Siegman B., 1982, A&AS 50, 451
Reshetnikov V.P., Hagen-Thorn V.A., Yakovleva V.A., 1993b, A&AS 99, 257
Reshetnikov V.P., Hagen-Thorn V.A., Yakovleva V.A., 1994, A&A 290, 693
Reshetnikov V.P., Combes F., 1994, A&A 291, 57 (RC94)
Reshetnikov V.P., Hagen-Thorn V.A., Yakovleva V.A., 1995, A&A 303, 398
Reshetnikov V.P., Hagen-Thorn V.A., Yakovleva V.A., 1996, A&A 314, 729
Reshetnikov V.P., Sotnikova N., 1997, A&A 325, 933
Reshetnikov V.P., Hagen-Thorn V.A., Yakovleva V.A., 1998, Astron. Reports 42, 439
Reshetnikov V.P., Evstigneeva E.A., 1999, Astron. Reports 43, 367
Richter O.-G., Huchtmeier W.K., 1987, A&AS 68, 427
Richter O.-G., Huchtmeier W.K., 1991, A&AS 87, 425
Richter O.-G., Sackett P.D., Sparke L.S., 1994, AJ 107, 99 (Paper I)
Rieke G.H., Cutri R.M., Black J.H., et al., 1985, ApJ 290, 116
Rodgers A.W., Peterson B.A., Harding P., 1978, ApJ 225, 768
Rood H.J., Dickel J.R., 1976, ApJ 205, 346
Rots A.H., 1980, A&AS 41, 189
Rigopoulou D., Lawrence A., White G.J., Rowan-Robinson M., Church S.E., 1996, A&A 305, 747
Rubin V.C., Burnstein D., Ford W.K., Thonnard N., 1985, ApJ 289, 81
Rubin V.C., 1987, in: Dark Matter in the Universe, IAU Symposium No. 117, Kormendy J. and Knapp G.R. (eds.). Reidel, Dordrecht, p. 51
Sackett P.D., Rix H.-W., Jarvis B.J., Freeman K.C., 1994, ApJ 436, 629
Sancisi R., Thonnard N., Ekers R.D., 1987, ApJ 315, L39
Sandage A., 1961, The Hubble Atlas of Galaxies. Carnegie Institution, Washington DC
Sanders D.B., Soifer B.T., Elias J.H., et al., 1988, 325, 74
Schechter P., Sancisi R., van Woerden H., Lynds C.R., 1984, MNRAS 208, 111
Schechter P.D., Huchra J.L., Tonry, 1993, PASP 105, 1470
Schneider S.E., Helou G., Salpeter E.E., Terzian Y., 1986, AJ 92, 742
Schweizer F., Whitmore B.C., Rubin V.C., 1983, AJ 88, 909
Schweizer F., 1987, ApJ 320, 454
Sekiguchi K., Wolstencroft R.D., 1993, MNRAS 263, 349
Shane W.W., 1980, A&A 82, 314
Shaw M., Axon D., Probst R., Gatley I., 1995, MNRAS 274, 369
Shostak G.S., 1978, A&A 68, 321
Sil'chenko O.K., 1998, A&A 330, 412
Silvergate P.R., Krumm N., 1978, ApJ 224, L98
Simien F., Prugniel P., 1997, A&AS 122, 521
Smith D., Herter T., Haynes M.P., Beichman C.A., Gautier T.N., 1995, ApJ 439, 623

Smith D.A., Herter T., Haynes M.P., Beichman C.A., Gautier T.N., 1996, ApJS 104, 217
Stanford S.A., Bushouse H.A., 1991, ApJ 371, 92
Staveley-Smith L., Davies R.D., 1988, MNRAS 231, 833
Staveley-Smith L., Norris R.P., Chapman J.M., et al., 1992, MNRAS 258, 725
Steiman-Cameron T.Y., Kormendy J., Durisen R.H., 1992, AJ 104, 1339
Strong A.W., Bloemen J.B.G.M., Dame T.M., et al., 1988, A&A 207, 1
Sulentic J.W., Arp H., 1983, AJ 88, 489
Theureau G., Bottinelli L., Coudreau-Durand N., et al., 1998, A&AS 130, 333
Thuan T.X., Martin G.E., 1981, ApJ 247, 823
Thuan T.X., Wadiak E.J., 1982, ApJ 252, 125
Tifft W.G., Cocke W.J., 1988, ApJS 67, 1
van den Broek A.C., van Driel W., de Jong T., et al., 1991, A&AS 91, 61
van Driel W., van den Broek A.C., de Jong T., 1991, A&AS 90, 55
van Driel W., Combes F., Casoli F., et al., 1995, AJ 109, 942
van Gorkom J.H., Schechter P., Kristian J., 1987, ApJ 314, 457
Vega J.C., Corsini E.M., Pizzella A., Bertola F., 1997, A&A 324, 485
Veilleux S., Kim D.-C., Sanders D.B., Mazzarella J.M., Soifer B.T., 1995, ApJS 98, 171
Vilchez J.M., Iglesia-Paramo J., 1998a, ApJS 117, 1
Vilchez J.M., Iglesia-Paramo J., 1998b, ApJ 506, L101
Wakamatsu K.-I., 1990, ApJ 348, 448
Weistrop D., Downes R.A., 1991, AJ 102, 1680
White S.D.M., Huchra J., Latham D., Davis M., 1983, MNRAS 203, 701
White R.L., Becker R.H., 1992, ApJS 79, 331
Whitmore B.C., McElroy B.C., Schweizer F., 1987, ApJ 314, 439
Whitmore B.C., Bell M., 1988, ApJ 324, 741
Whitmore B.C., Lucas R.A., McElroy D.B., et al., 1990, AJ 100, 1489 (PRC)
Whitmore B.C., 1991, A few statistics from the Catalogue of PR galaxies, in: Casertano S., Sackett P., Briggs F. (eds.) Warped Disks and Inclined rings around Galaxies. Cambridge University press, p. 60
Wootten H.A., Armstrong J.T., Hartman L., 1983 (priv. comm.) (see Huchtmeier & Richter 1989)
Wright G.S., Joseph R.D., Meikle W.P.S., 1984, Nat 309, 430
Wunderlich E., Klein U., 1991, ApJS 87, 247
Zabludoff A.I., Geller M.J., Huchra J.P., Vogeley M.S., 1993, AJ 106, 1273
Zhou S., Wynn-Williams C.G., Sanders D.B., 1993, ApJ 409, 149